Science
AAAS

# Supplementary Materials for

## Chemically recyclable polyolefin-like multiblock polymers

Yucheng Zhao *et al*.

Corresponding author: Garret M. Miyake, garret.miyake@colostate.edu

*Science* **382**, 310 (2023)
DOI: 10.1126/science.adh3353

**The PDF file includes:**

## Materials and Methods

### Materials

Oxacycloheptadec-10-en-2-one (ambrettolide) was purchased from Perfumer Supply House. Lithium aluminum hydride (LAH), *cis*-cyclooctene (COE), N-bromosuccinimide (NBS), azobisisobutyronitrile (AIBN), magnesium turnings, cuprous iodide (CuI), potassium t-butoxide were purchased from Sigma Aldrich. 1-bromohexane was purchased from Oakwood Chemicals. (H2IMes) (PPh3) (Cl)2RuCHPh (Grubbs II) was purchased from Umicore. Carbonylchlorohydrido[6-(di-t-butylphosphinomethyl)-2-(N,N-diethylaminomethyl)pyridine]-ruthenium(II) (Milstein catalyst precursor, **Ru-1** in this work) and carbonylchlorohydrido{bis[2-(diphenylphosphinomethyl)ethyl]amino}ethyl]amino}ruthenium(II) (Ru-MACHO, **Ru-2** in this work) were purchased from Strem Chemicals and used without further purification. Anhydrous anisole, anhydrous diethyl ether, tetrahydrofuran (THF), toluene, isopropanol, cyclohexane, and other solvents were purchased from Sigma Aldrich or Fisher. Tetrahydrofuran and toluene were obtained and purified using an mBraun MB-SPS-800 solvent purification system and kept under a nitrogen atmosphere. *Cis*-cyclooctene was dried by stirring over calcium hydride, distilled under vacuum, then transferred to amber vials in a nitrogen filled glovebox. High-density polyethylene (HDPE) (melt flow index = 2.2 g/10 min,190 °C/2.16 kg, $M_n$ = 17.2 kDa, $M_w$ = 92.2 kDa, $Đ$ = 5.4) and linear low-density polyethylene (LLDPE) (melt flow index = 1.0 g/10 min, 190 °C/2.16 kg, $M_n$ = 31.8 kDa, $M_w$ = 90.4 kDa, $Đ$ = 2.8) were purchased from Sigma Aldrich and used without further purification.

### Methods

Nuclear magnetic resonance (NMR) spectra were obtained using a Bruker 400 MHz NMR Spectrometer at 298 K and a Varian 500 MHz NMR Spectrometer at 383 K. All $^1$H NMR experiments are reported in parts per million (ppm) and were measured relative to the signals for residual chloroform (δ = 7.26 ppm) in deuterated chloroform, toluene (δ = 2.09 ppm) in deuterated toluene, and tetrachloroethane (δ = 6.00 ppm) in deuterated tetrachloroethane. $^{13}$C NMR quantitative spectra were obtained at 403 K and reported in ppm are relative to tetrachloroethane (δ = 73.78 ppm) and were obtained with $^1$H decoupling.

Size exclusion chromatography molecular weight determination: High Temperature Size Exclusion Chromatography (HT-SEC) analysis of the polymer samples were performed using a Tosoh EcoSec HLC-8321 High Temperature SEC System with autosampler and a differential refractive index (DRI) detector. The mobile phase used was 1,2,4-Trichlorobenzene (TCB) (Fischer Scientific-HPLC Grade) which was used as-received with no inhibitor added. Polymer separation was performed using four (4) Tosoh TSKgel columns in the following order: TSKgel guard column (HHR (30) HT2 7.5 mm I.D. x 7.5 cm., PN 22891), TSKgel GMHHR (20) HT2 (7.8 mm I.D. x 30 cm columns, PN 22888), and two sequential TSKgel G2000 columns (HHR (20) HT2 7.8 mm I.D. x 30 cm columns, PN 22890). Additionally, a reference column, specifically a TSKgel GMH HR-H (S) HT2 (7.8 mm I.D. x 30cm column, PN 22889) was used. Tosoh's Polystyrene-Quick Kit-M (PN 21916) was used to create the calibration curve from a series of polystyrene (PS) standards including: Tosoh PS F-10 ($M_w$ = 106,000 Daltons (Da) – P/N 05210)) , PSS Polymer ($M_w$= 66,000 Da – Batch No: ps14057), Wyatt ($M_w$ = 30,000 Da – P/N P8402-03001), and PSS Polymer ($M_w$ = 1,200 Da – Batch No: ps14057). The solvent stock was set to 40

°C while the pump oven was set to 50 °C. The columns, RI detector, injector valve, and autosampler were all set to 160 °C. Samples were prepared in Tosoh 10 mL high temperature sample vials with PTFE caps. 6-20 mg of sample were placed in a Tosoh high temperature 26 µm stainless steel mesh filter and TCB solvent was added to reach an end concentration of ~1.7 mg/mL and heated on the autosampler for two hours with occasional agitation. Samples were injected into a 300 µL sample loop and ran at an operating flow rate of 1.0 mL/min for the sample columns. Meanwhile, the reference column was set to an operating flow rate of 0.5 mL/min. Run times for all standards and samples was 60 minutes. Eco-Sec 8321 software (Tosoh) was used for data processing. All higher molecular weight sample peaks (>10,000 Da) were integrated in the range of when they first deviated from baseline to 2,000 Da end point. All lower molecular weight sample peaks (<10,000 Da) were integrated in the range of when they first deviated from baseline to 500 Da endpoint. Mark Houwink correction values were applied to the polystyrene calibration curve. Mark Houwink values used for polystyrene were K = 12.1 x 10-5 dL/g and Alpha = 0.707. Mark Houwink values used for polyethylene were K = 40.6 x 10-5 dL/g and Alpha = 0.725.

Differential scanning calorimetry (DSC) measurements were performed using a TA Instruments Auto Q20 in $N_2$ atmosphere. All values of $T_m$, $T_g$ and $\Delta H_f$ were obtained from the second heating cycle. All cycles used heating and cooling rates of 10 °C/min. Degrees of crystallinity were calculated from $\Delta H_f$ integrations compared to the equilibrium heat of fusion for fully crystalline polyethylene of relevant molecular weight ($M_w$ = 60.7 kDa).

Thermogravimetric Analysis (TGA) was performed using a Mettler-Toledo TGA/SDTA851. Samples were heated in platinum pans from ambient temperatures to 500 °C using a heating rate of 10 °C/min under $N_2$ purge.

Wide-Angle X-Ray Scattering (WAXS) data was collected using a Bruker D-8 Discover DaVinci X-ray diffractometer (Cu-Kα X-ray source, line focus) in transmission. A 0.6 mm divergent slit was placed on the primary beam side and a high-resolution energy-dispersive LYNXEYE-XE-T detector on the diffracted beam side during the WAXS measurements. WAXS measurements were performed with soller slits on the primary and diffracted beam side (2.5° separation). The instrument alignment was verified with NIST 1976b SRM.

Rheological tests were conducted using a TA Instruments DHR-2 rheometer with 8 mm parallel plate geometry under nitrogen purge. The samples were compression molded into circular discs of 8 mm in diameter and approximately 1.0 mm in height. Using a gap height of 900 µm, step (transient) creep tests were conducted at a constant temperature of 150 °C, applying a stress of 20.0 Pa with a nitrogen atmosphere. Each test lasted for a duration of 10000 seconds.

Dynamic Mechanical Thermal Analysis (DMTA) was conducted on a TA Instruments Q800 DMA Analyzer equipped with a liquid nitrogen GCA tank attachment. Sample length was measured upon loading within the grips by Q-series measurement software. Tests were performed at 1 Hz and 0.2% strain, starting at –125 °C and heated at rate of 3 °C/min.

Tensile tests were performed on an Instron 5966 Universal Testing System equipped with a 10 kN load cell using a crosshead speed of 5 mm/min until sample failure. Specimens were prepared according to ASTM D638 for Type-V standard tensile bar specimens (cross-section w = 3.18 mm). Tensile tests for only sample **PE0** were performed using an Instron 4442 Universal Testing System equipped with a 50 N load cell, using a crosshead speed of 5 mm/min until sample failure. Material Toughness ($U_T$; MJ $m^{-3}$) was determined by integration of the tensile curve. Tensile statistics were

reported according to the average and standard deviation (to one significant figure) of all tensile tests, typically between four to six specimens per sample.

Polarized Light Optical Microscopy (PLOM) Images were collected on a Keyence VHX-6000 digital microscope with a polarizer lens. Samples were prepared by heating between glass slides at 200 °C for 20 minutes, then cooled at a rate of ~1.4 °C/minute to room temperature while under modest compression of ~6 psi. A manual Carver 3912 Press was utilized for heating and application of pressure.

Melt compressed films were prepared using a Carver Auto Series Plus Laboratory Press (Model 3889.1PL1000, Max Force 15 ton) at a force of 3,000 lbs (resultant pressure of 175.2 psi) and temperature of 150 °C for 10-20 minutes. All samples were cooled to room temperature at a rate of ~30 °C/min while still under compression.

Density measurements were performed at 20 °C using a Mettler-Toledo XSR205DU Analytical Balance equipped with a Mettler Toledo gravimetric density kit, using reference solvent of absolute anhydrous Ethyl Alcohol (density 0.7892 g/mL at 20 °C), 200 proof purchased from PHARMCO by Greenfield Global.

Elemental concentrations of Ru were measured using an NexION 350D mass spectrometer (PerkinElmer, Branford, CT) connected to a PFA-ST (Elemental Scientific, Omaha, Nebraska) nebulizer and a peltier controlled (PC3x, Elemental Scientific) quartz cyclonic spray chamber (Elemental Scientific) set at 4°C. Samples were introduced using prepFAST SC-2 (Elemental Scientific) autosampler. Prior to analysis the nebulizer gas flow and Quadrupole Ion Deflector (QID) were optimized for maximum Indium signal intensity. A daily performance check was also run which ensured that the instrument was operating properly and obtained a $CeO^+$:$Ce^+$ less than 0.025 and a $Ce^{++}$:Ce of less than 0.030. A calibration curve was prepared in Milli Q water by serial dilution of commercially available single-element ICP-MS stock solutions. Internal standard solution consisting of a final concentration of 10 µg/L of Ir, 10 µg/L Rh and 2500 µg/L $^6$Li were infused to each sample during analysis. A pool quality control (QC) solution consisting of equal volume of each unknown sample was run every 5$^{th}$ sample. Data was processed using Excel. Ru analysis was subjected to internal standard corrections and subsequently drift corrected (*35*). Corrections were chosen based on minimizing the coefficient of variance (CV) for the QC samples. Limits of detection (LOD) and limits of quantification (LOQ) were calculated as 3 times or 10 times the standard deviation of the blank divided by the slope of the calibration curve respectively. Final concentrations are given in µg/g. Measured calculations below the LOD were assigned as <LOD.

General procedure for the synthesis of CTA (Fig. S1).

To a 500 mL round bottom flask with a stir bar was charged with lithium aluminum hydride (LAH, 22.8 g, 0.601 mol) and THF (250 mL) in an ice bath. The ambrettolide (53.2 g, 0.211 mol) in 100 mL THF was dropwise added to the solution with vigorous stirring. The reaction was stirred at room temperature for 12 h. Then the reaction was cooled to 0 °C using an ice bath and quenched by adding 23.0 mL water, NaOH solution (15 wt% in water, 23.0 mL), and an additional 23.0 mL water. The slurry was filtered and washed with EtOAc. The filtrate was collected, dried over sodium sulfate, filtered, and concentrated to afford the product as a white solid (42.1 g, 82.0 % yield). $^1$H NMR (400 MHz, CDCl3) δ = 5.38–5.36 (m, 2H), 3.62 (t, *J* = 6.8 Hz, 4H), 1.99–1.93 (m, 4H), 1.58–1.51 (m, 4H), 1.36–1.25 (m, 16H) ppm; $^{13}$C NMR (100 MHz, $CDCl_3$) δ = 130.6, 130.4, 63.1, 32.9, 32.9, 32.7, 32.6, 29.7, 29.7, 29.6, 29.5, 29.1, 29.0, 25.8, 25.7 ppm.

General procedure for the synthesis of oligomers (Fig. S2) (*36*).

In a $N_2$ filled glovebox, a stock solution of catalyst was prepared by dissolving Grubbs II (76.5 mg, 0.09 mmol) and *cis*-hexadec-6-ene-1,16-diol (**CTA**, 119 mg, 0.464 mmol) in 1.20 mL THF and stirred for 10 min. A 500 mL Schlenk flask with a stir bar was charged with **CTA** (3.84 g, 15.0 mmol), monomer (150 mmol) and THF (100 mL). 1.00 mL catalyst solution was added into the flask. Then the flask was sealed, taken out of glovebox, and stirred at 40 °C for 5 h. The flask was cooled to room temperature before ethyl vinyl ether (650 mg, 9.01 mmol) was added and stirred into the solution for 5 min to quench the reaction. A small aliquot was taken to analyze the conversions of **CTA** and monomer by $^1$H NMR, which was measured to be over 95%. The solution was concentrated under vacuum to afford the unsaturated oligomers, which were analyzed by HT-SEC and $^1$H NMR to give the $M_{n,\,SEC}$.

To hydrogenate the oligomers, the oligomers (see sections **HO-HB-OH** and **HO-SB-OH**) were dissolved in THF (100 mL) and transferred to a pressure reactor. The reactor was sealed and cycled 4 times with 20 bar $H_2$, and then charged with 40 bar $H_2$. The reactor was heated to 100 °C, and stirred at 100 rpm for 12 h. The reactor was cooled to room temperature, recharged with $H_2$ to 40 bar, and heated to 100 °C and reacted for 24 h. After cooling to room temperature, the reactor was depressurized, and the chamber flushed with nitrogen.

**HO-HB-OH** (Fig. S3)**:** *cis*-cyclooctene (16.53 g, 0.150 mol) was used as the monomer. After polymerization and hydrogenation, the mixture was washed with THF and dried under vacuum at 100 °C for 24 h to afford 13.52 g white solid as the hard block **HO-HB-OH**. The $M_{n,NMR}$ of hydrogenated **HO-HB-OH**, calculated by $^1$H NMR (in toluene-d8, 383 K) based on the Fig. S3, is 1.5 kDa. SEC (TCB, 160 °C) $M_n$ = 1.9 kDa, $M_w$ = 3.3 kDa, $Đ$ = 1.7.

**HO-SB-OH** (Fig. S4)**:** 3-hexylcyclooctene was synthesized based on the literature (*37, 38*) (29.15 g, 0.150 mol) and used as the monomer. After polymerization and hydrogenation, the mixture was precipitated from methanol, dried under vacuum at 100 °C for 24 h to afford 21.53 g colorless oil as the soft block **HO-SB-OH**. The $M_{n,NMR}$ of hydrogenated oligomer calculated by $^1$H NMR (in $CDCl_3$, 298 K) based on the Fig. S4 is 2.3 kDa. SEC (TCB, 160 °C) $M_n$ = 1.8 kDa, $M_w$ = 3.0 kDa, $Đ$ = 1.7.

General procedure for copolymerization of multiblock copolymers.

*Preparation of catalyst solution:*

In a $N_2$ atmosphere glovebox, carbonylchlorohydrido[6-(di-*t*-butylphosphinomethyl)-2-(*N,N*-diethylaminomethyl)pyridine]ruthenium(II) (9.8 mg, 0.02 mmol) and potassium *tert*-butoxide (8.8 mg, 0.08 mmol) were combined in a 10 mL vial with a stir bar. 9.8 mL anisole was added and the mixture was stirred for 10 minutes at room temperature.

*Polymerization:*

The corresponding ratios of **OH-HB-OH** and **OH-SB-OH** (1.00 mmol in total) as described in the Table S2 were dried in a 50 mL Schlenk tube at 130 °C under vacuum for 2 h. Under $N_2$ flow, a 9.8 mL solution of carbonylchlorohydrido[6-(di-*t*-butylphosphinomethyl)-2-(*N,N*-diethylaminomethyl)pyridine]ruthenium(II) (1.00 mg/mL, 1.00 mol% to the -OH bond) in anisole was added to the tube via a syringe and the temperature was raised to 150 °C with stirring. The mixture was stirred for 48 h. After 48 h, the mixture was diluted with 25 mL xylenes at 140 °C,

precipitated in isopropanol (150 mL) and filtered to give the multiblock copolymers. The isolated copolymers were dried under vacuum at 130 °C for 24 h.

General procedure for depolymerization of multiblock copolymers.

In a $N_2$ filled glovebox, the carbonylchlorohydrido[6-(di-*t*-butylphosphinomethyl)-2-(*N,N*-diethylaminomethyl)pyridine]ruthenium(II) (36.0 mg, 0.074 mmol) and potassium tert-butoxide (32.0 mg, 0.285 mmol) were combined in a 50 mL vial with a stir bar. 36.0 mL toluene was added and the mixture was stirred for 10 minutes at room temperature. 1.00 mmol PE copolymers was added to a 100 mL beaker with a stir bar. 0.500 eq (relative to ester bond) of potassium tert-butoxide and a solution of catalyst (1.00 mg/mL, 2.50 mol% to the ester bond) were added to the beaker. The beaker was taken out of glovebox and put in a pressure reactor. The reactor was sealed and cycled 4 times with 20 bar $H_2$, and then charged with 40 bar $H_2$. Then, the reactor was heated to 150 °C for 72 h (or 160 °C for 24 h). After cooling to room temperature, the reactor was depressurized, and the chamber flushed with nitrogen. A small aliquot was taken to determine the conversion by $^1$H NMR.

Excess hexanes was added to the beaker, and the mixture was stirred for 30 minutes and centrifuged to separate the solid and the solution. The solid was washed with hexanes, centrifuged (6000 rpm, 10 minutes, 3 cycles) and recrystallized in toluene and filtered to give hard blocks. The corresponding solutions and supernatants were combined and concentrated. The residue was purified by flash chromatography (eluting with THF) on silica gel to give soft blocks.

Removal of Ru catalyst from the polymers.

Method A: 1.00 g polymer and 100 mL xylene were combined in a 500 mL flask. After the polymer was completely dissolved at 140 °C, the solution was precipitated in 200 mL THF with vigorously stirring. The precipitation was repeated three times and the solid was dried under vacuum for 24 h to give the polyolefin.

Method B: 1.00 g polymer and 100 mL xylene were combined in a 500 mL flask. After the polymer was completely dissolved at 140 °C, the solution was cooled to room temperature. And the solid was filtered and washed with THF. The recrystallization was repeated three times and the solid was dried under vacuum for 24 h to give the polyolefin.

Method C: 1.00 g polymer was dissolved in the 100 mL xylene at 135 °C. Then, the temperature turned to 90 °C. When the temperature was stabilized, 2.00 mmol 2-aminoethanethiol (coordinating ligand) was added. After 30 mins, the solution was precipitated into isopropanol to afford white solid. The solid was washed with isopropanol 3 times and dried under vacuum for 24 h.

Method D: The soft block was purified by flash chromatography (eluting with THF) on silica gel.

The purified samples were analyzed by ICP-MS to determine the residual Ru in the copolymers.

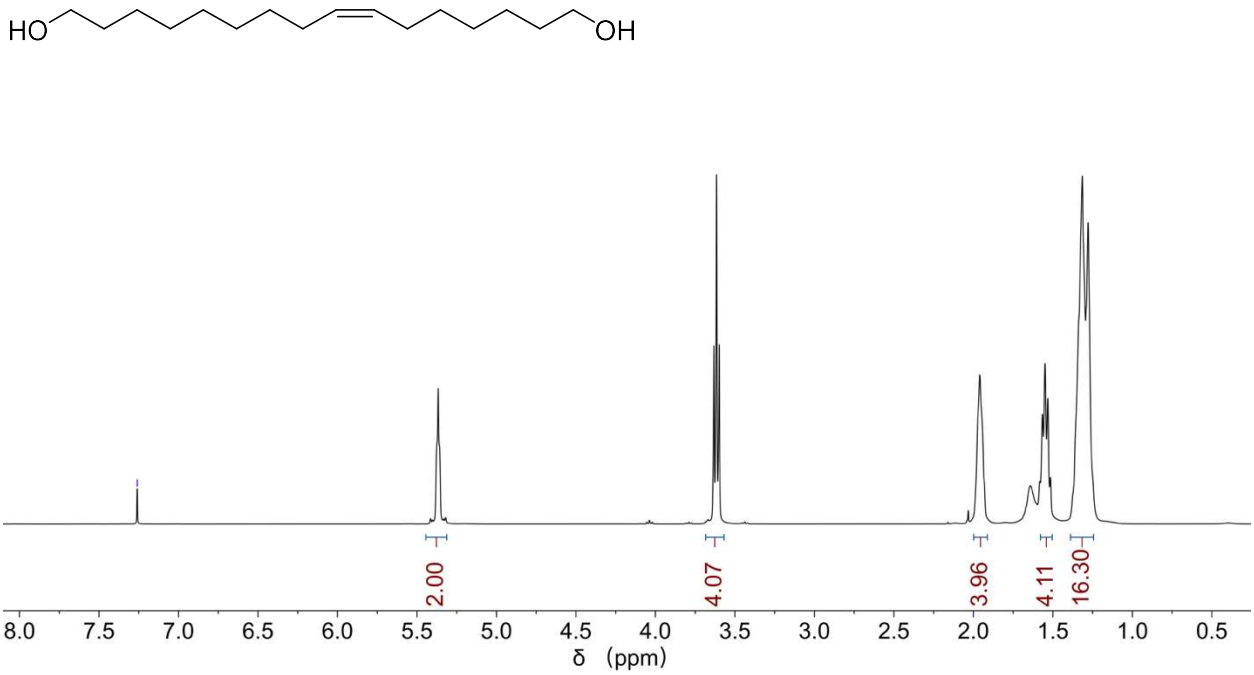


**Fig. S1.** $^{1}$H NMR spectrum (298 K, 400 MHz, $CDCl_3$) of *cis*-hexadec-6-ene-1,16-diol (**CTA**).

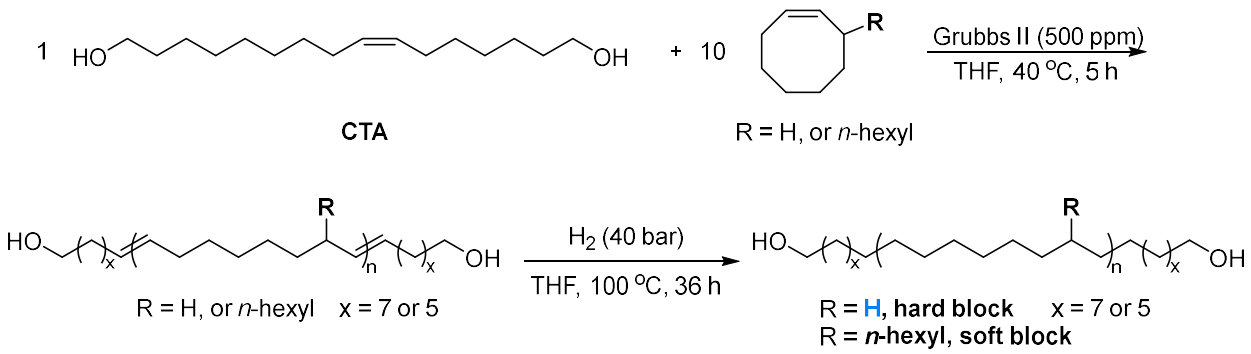


**Fig. S2.** Synthetic route for hard block and soft block. The residual Grubbs II was used for hydrogenation. (*36*)

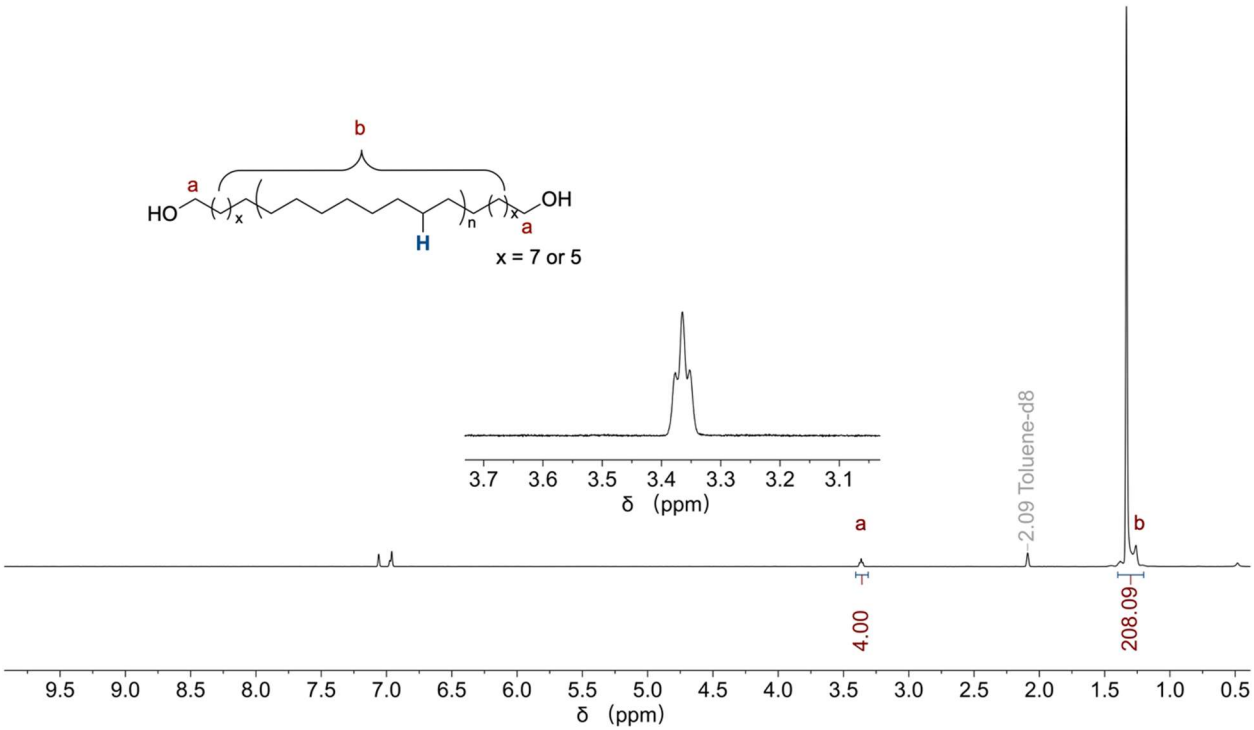


**Fig. S3.** $^{1}$H NMR spectra (373 K, 500 MHz, Toluene-d8) of hard block **HO-HB-OH** (hydrogenated HO-poly(cyclooctene)-OH).

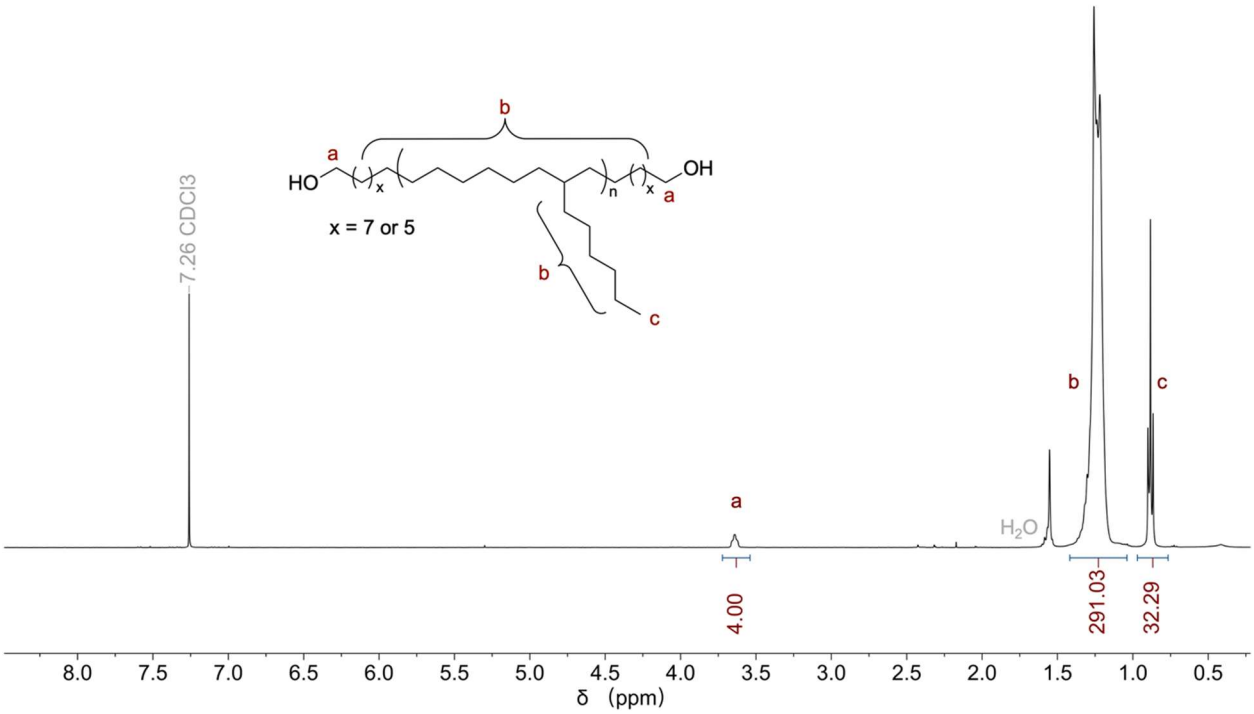


**Fig. S4.** $^{1}$H NMR spectrum (298 K, 400 MHz, $CDCl_3$) of soft block **HO-SB-OH** (hydrogenated HO-poly(3-hexylcyclooctene)-OH).

Calculation of degree of branching and branching numbers in copolymers.

$$\text{C6 branching (mol\%)} = \frac{I_1/3}{(I_2+I_1/3)/2 + I_3/2 + I_4 + I_5/2 + I_6/2 + I_1/3} \times 100\%$$

The branching numbers (per 1000C) was calculated based on the equation:

$$\text{Branching number (per 1000C)} = \frac{I_1/3}{(I_2+I_1/3)/2 + I_3/2 + I_4 + I_5/2 + I_6/2 + I_1/3} \times 1000$$

Equation **S1**

Where $((I_2 + I_1/3) + I_3 + 2I_4 + I_5 + I_6)$ is the integration of $-CH_2-$ in the copolymers, (an additional $I_4$ needs to be counted because 2 equivalents of $-CH_2OH$ were converted to 1 equivalent of $-COOCH_2-$), and $I_1$ is the integration of $-CH_3$ (C6 branching) in the copolymers. Hard (%) is the molar ratio of hard block in copolymers.

The degree of branching and branching number in copolymers can be calculated based on Fig. S5–S10.

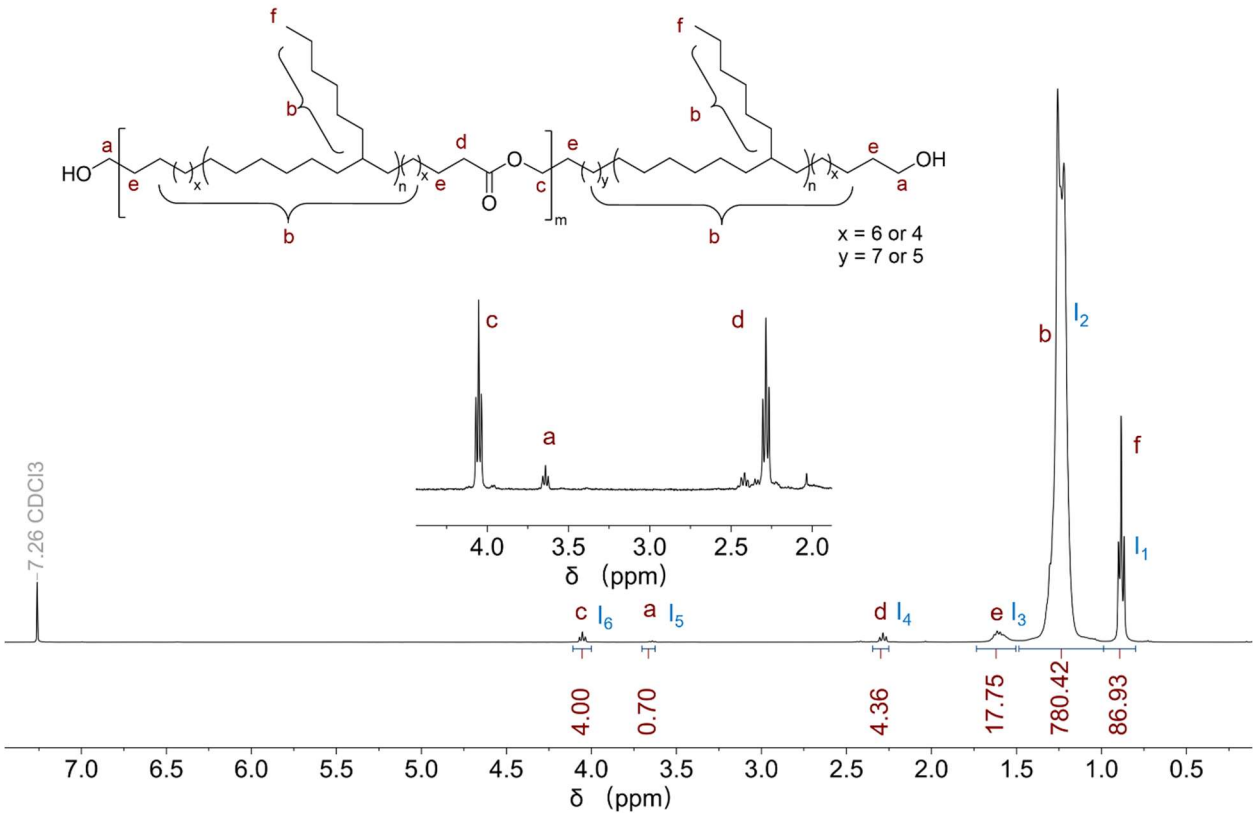


**Fig. S5.** $^1$H NMR spectra (298 K, 400 MHz, $CDCl_3$) of **PE0** (0% hard blocks).

Calculation of hard block (mol%) in copolymers.

The hard block (mol%) in copolymers can be calculated by:

$$\text{Hard (\%)} = \frac{\text{n (hard)}}{\text{n (hard)} + \text{n (soft)}} \times 100\%$$

The ratio of -$CH_2$- to the -$CH_2OH$ (Fig. S3) for the hard block can be calculated based on the ratio of integration of $H_b$ (208.09) and $H_a$ (4.00) as 52.02.

The ratio of -$CH_2$- to -$CH_3$ (Fig. S4) in soft block can be calculated based on the ratios of integration of $H_b$ (291.03) and $H_c$ (32.29), which is 9.01. And the ratio of -$CH_3$ to the -$CH_2OH$ (Fig. S4) can be calculated based on the ratio of integration of $H_b$ (32.29) and $H_a$ (4.00) as 8.07.

For calculating hard block (mol%) in copolymers, the hard block can be calculated based on the equation:

$$\text{Hard (\%)} = \frac{(I_2 + I_3 - I_1 \times 9.01)/52.02}{(I_2 + I_3 - I_1 \times 9.01)/52.02 + I_1/8.07} \times 100\% \qquad \text{Equation } \mathbf{S}2$$

Where ($I_2 + I_3$) is equal to the integration of -$CH_2$- from oligomers, and $I_1$ is the integration of -$CH_3$ (C6 branching) in the copolymers. Hard (%) is the molar ratio of hard block in copolymers. The hard block (mol%) and branching number in copolymers can be calculated based on Fig. S5 – S9.

Calculation of ester bond (-$CO_2$-, per 1000 carbons) in copolymers.

The $CO_2$ per 1000 C in copolymers can be calculated based on the equation:

$$CO_2 \text{ per } 1000C = \frac{(I_4+I_6)/4}{I_5/2 + (I_2 + I_1/3)/2 + I_1/3 + I_6/2 + I_4 + I_3/2} \times 1000 \qquad \text{Equation } \mathbf{S}3$$

Where ($I_4$+$I_6$)/2 is the average integration of ester bond ($CO_2$) in the copolymers, and ($I_4$+$I_6$)/4 is equal to the carbon integration of $CO_2$. The sum of the integration of chain end -$CH_2$- ($I_5$/2), -$CH_2$- (($I_2$ + $I_1$/3)/2, -$CH_3$ ($I_1$/3), main chain -$CH_2OO$- ($I_6$/2), main chain -$CH_2COO$- ($I_4$), and $\beta$-$CH_2$ adjacent to ester bond ($I_3$/2) represents the integration of the total carbon in copolymers. The $CO_2$ per 1000C data for **PE0**–**PE100** were calculated based on Fig. S5–S10 and presented in Table S2.

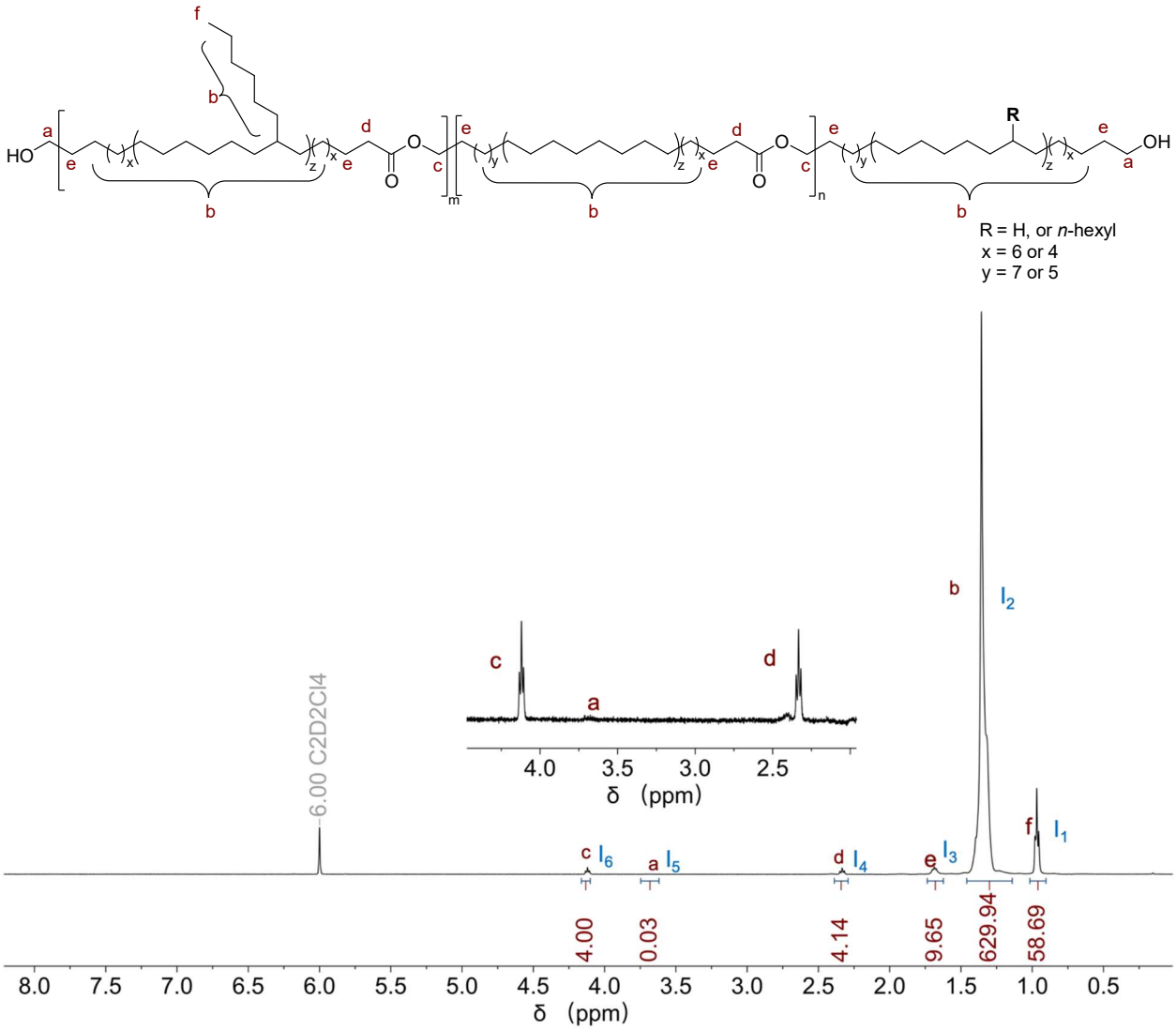


**Fig. S6.** $^{1}$H NMR spectra (383 K, 500 MHz, tetrachloroethane-d2) of **PE20** (20% hard blocks).

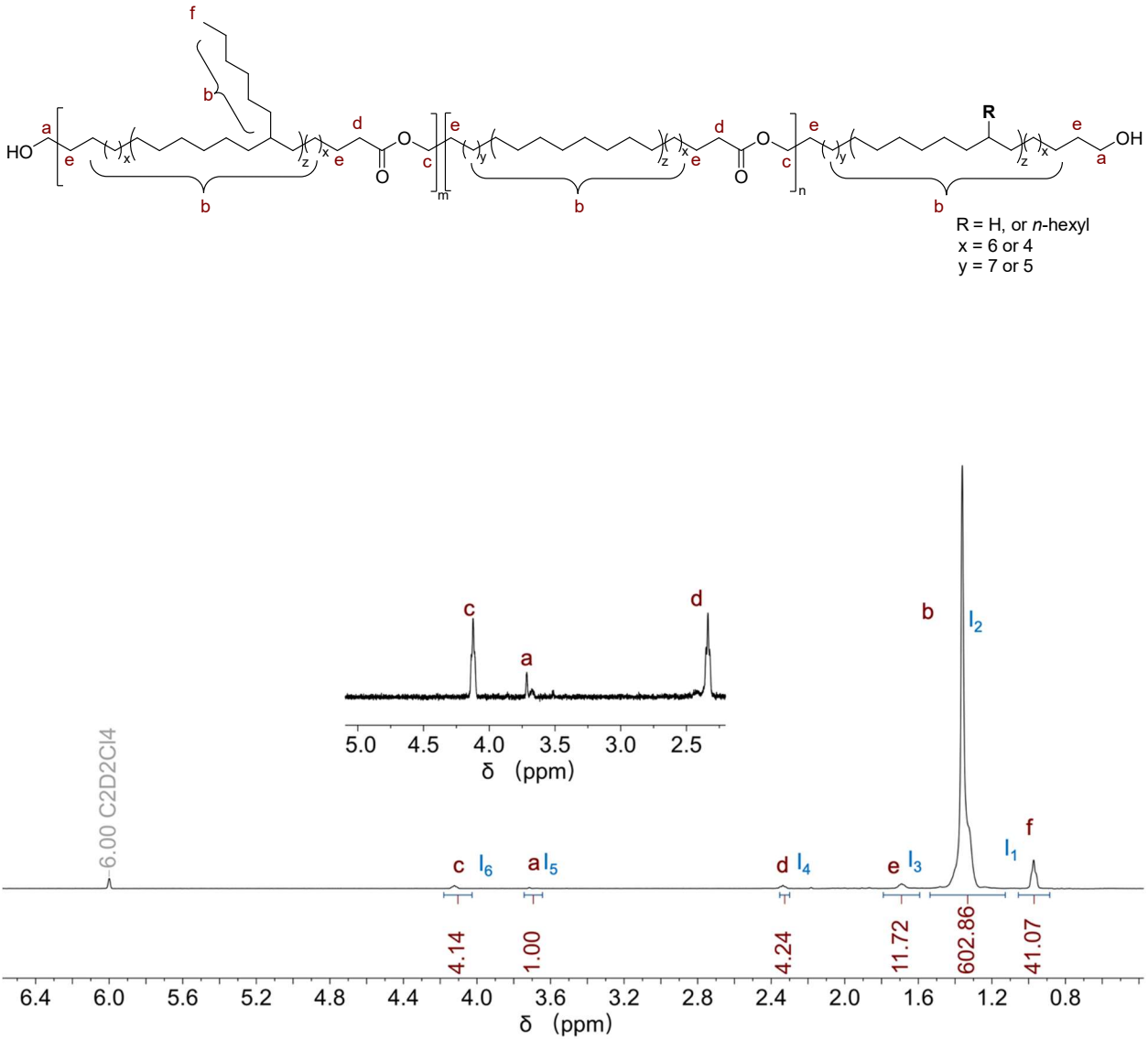


**Fig. S7.** $^{1}$H NMR spectra (383 K, 500 MHz, tetrachloroethane-d2) of **PE40** (40% hard blocks).

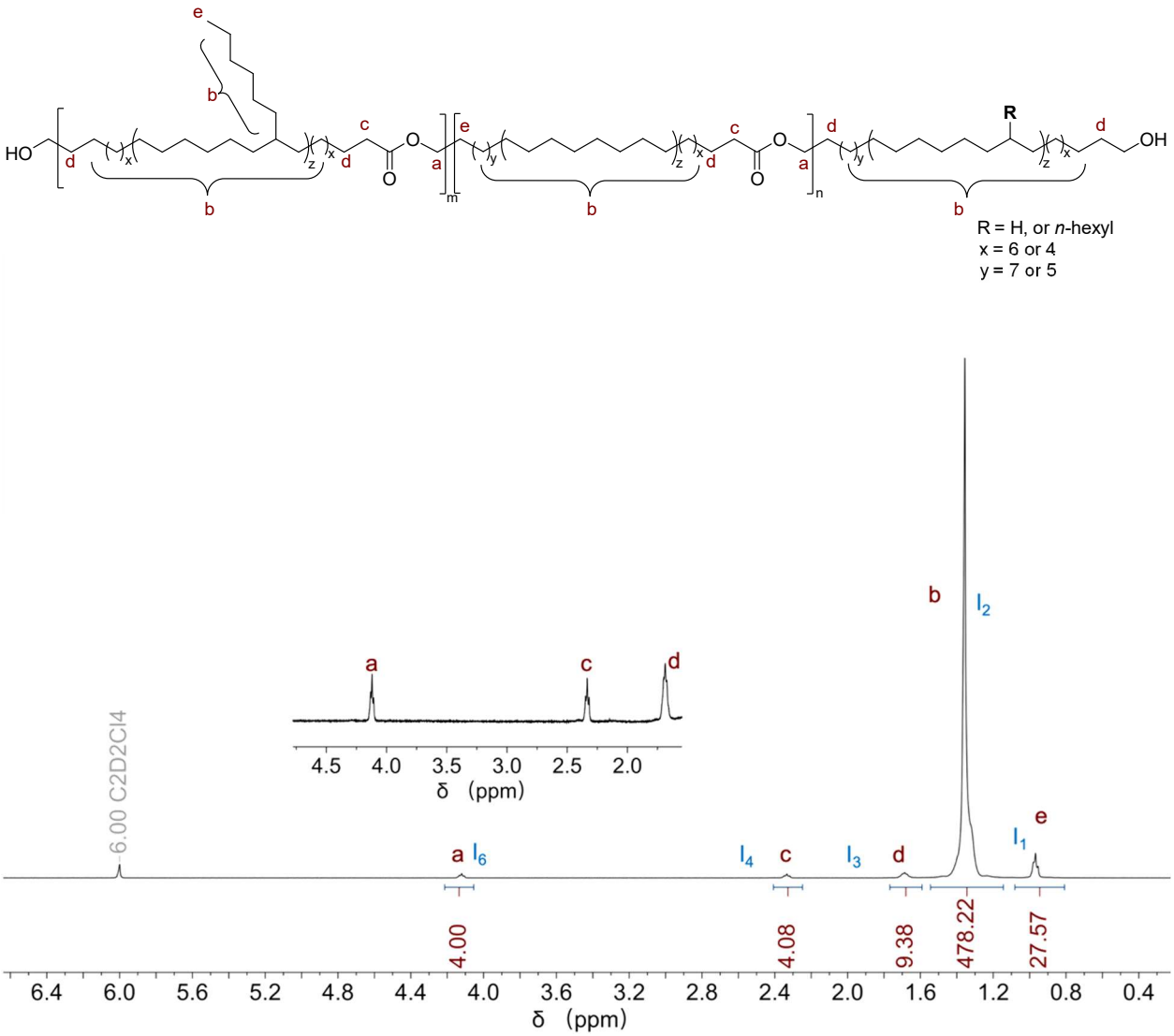


**Fig. S8.** [1]H NMR spectra (383 K, 500 MHz, tetrachloroethane-d2) of **PE60** (60% hard blocks).

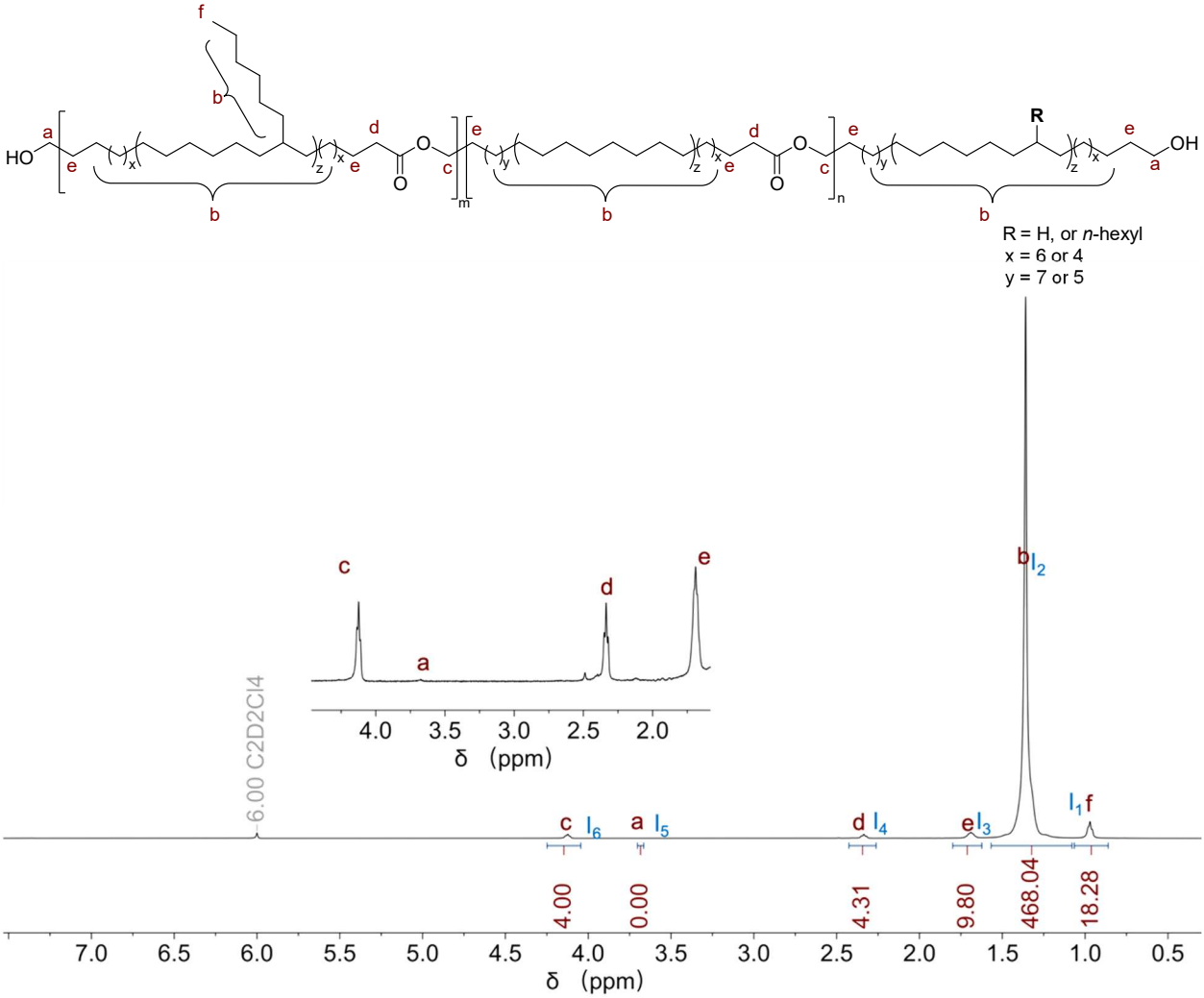


**Fig. S9.** $^{1}$H NMR spectra (383 K, 500 MHz, tetrachloroethane-d2) of **PE80** (80% hard blocks).

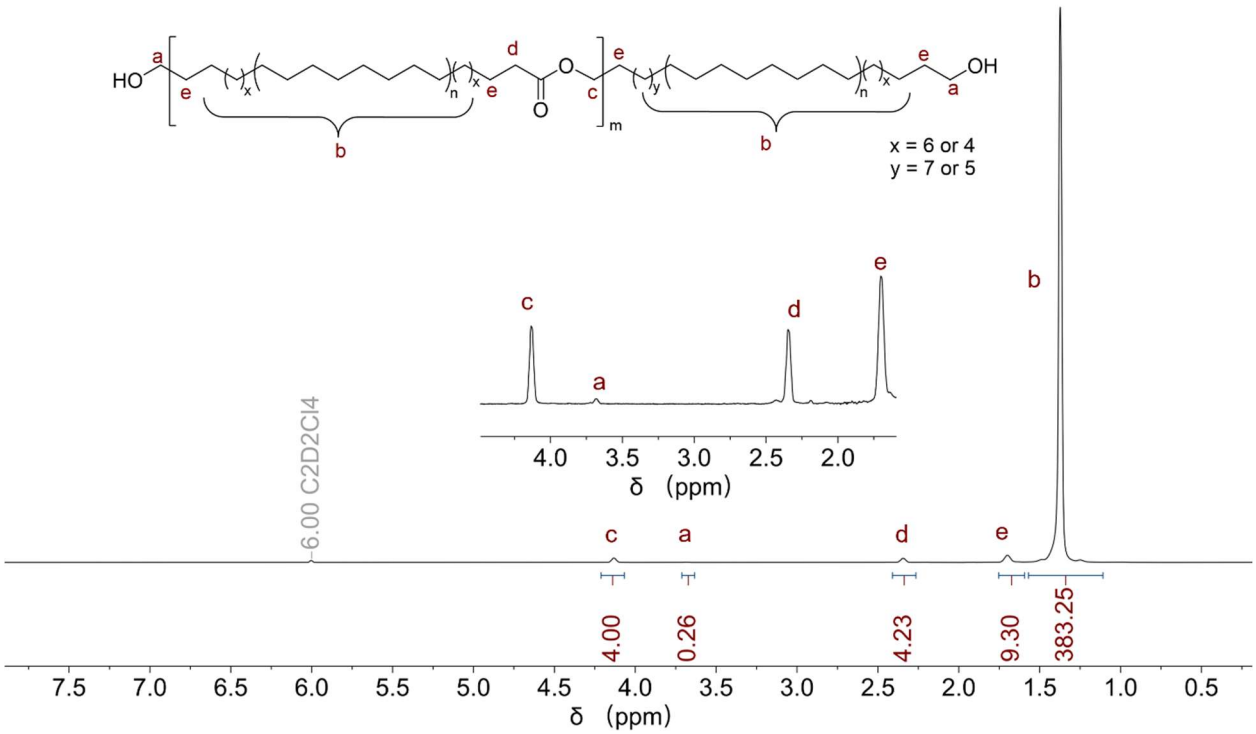


**Fig. S10.** $^{1}$H NMR spectra (383 K, 500 MHz, tetrachloroethane-d2) of **PE100** (100% hard blocks).

Characterization of oligomers.

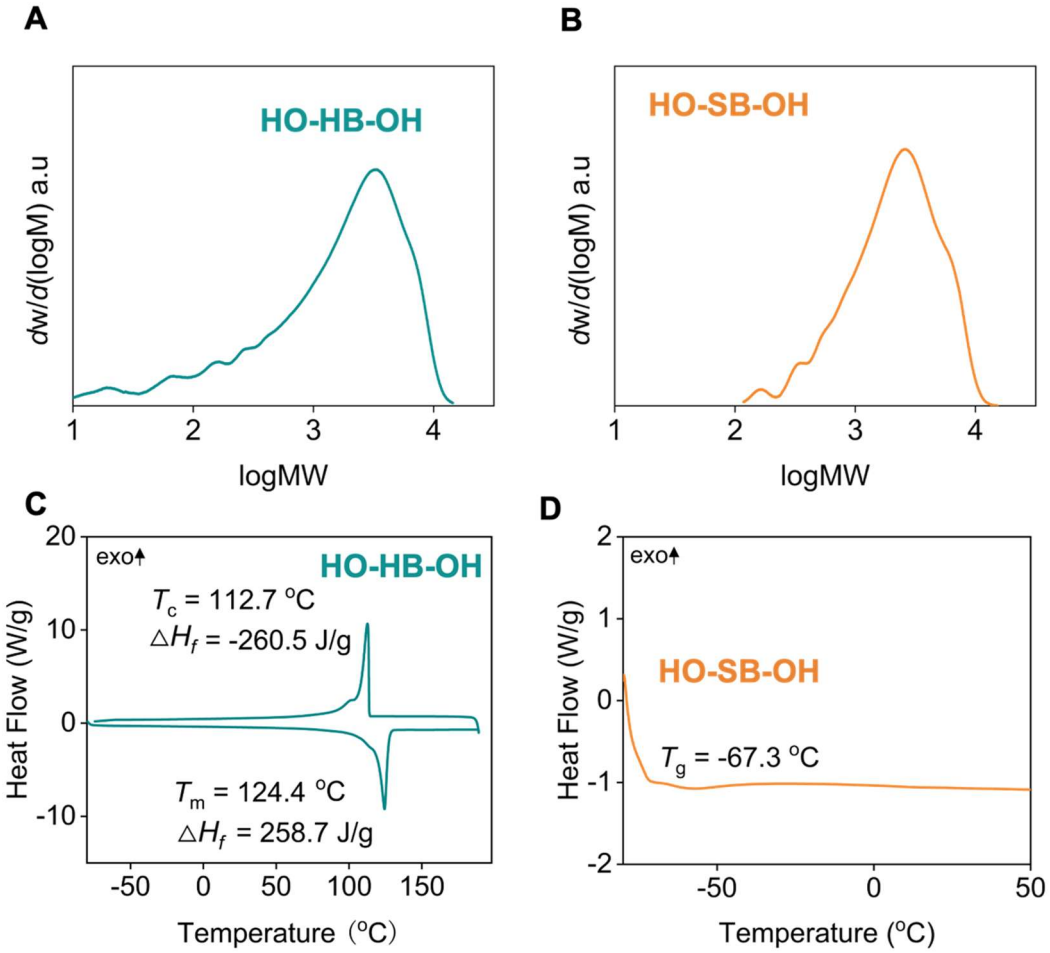


**Fig. S11.** The HT-SEC (TCB at 160 °C) traces of (A) **HO-HB-OH** and (B) **HO-SB-OH**. DSC traces of (C) **HO-HB-OH** and (D) **HO-SB-OH**.

Characterizations of copolymers, HDPE, and LLDPE.

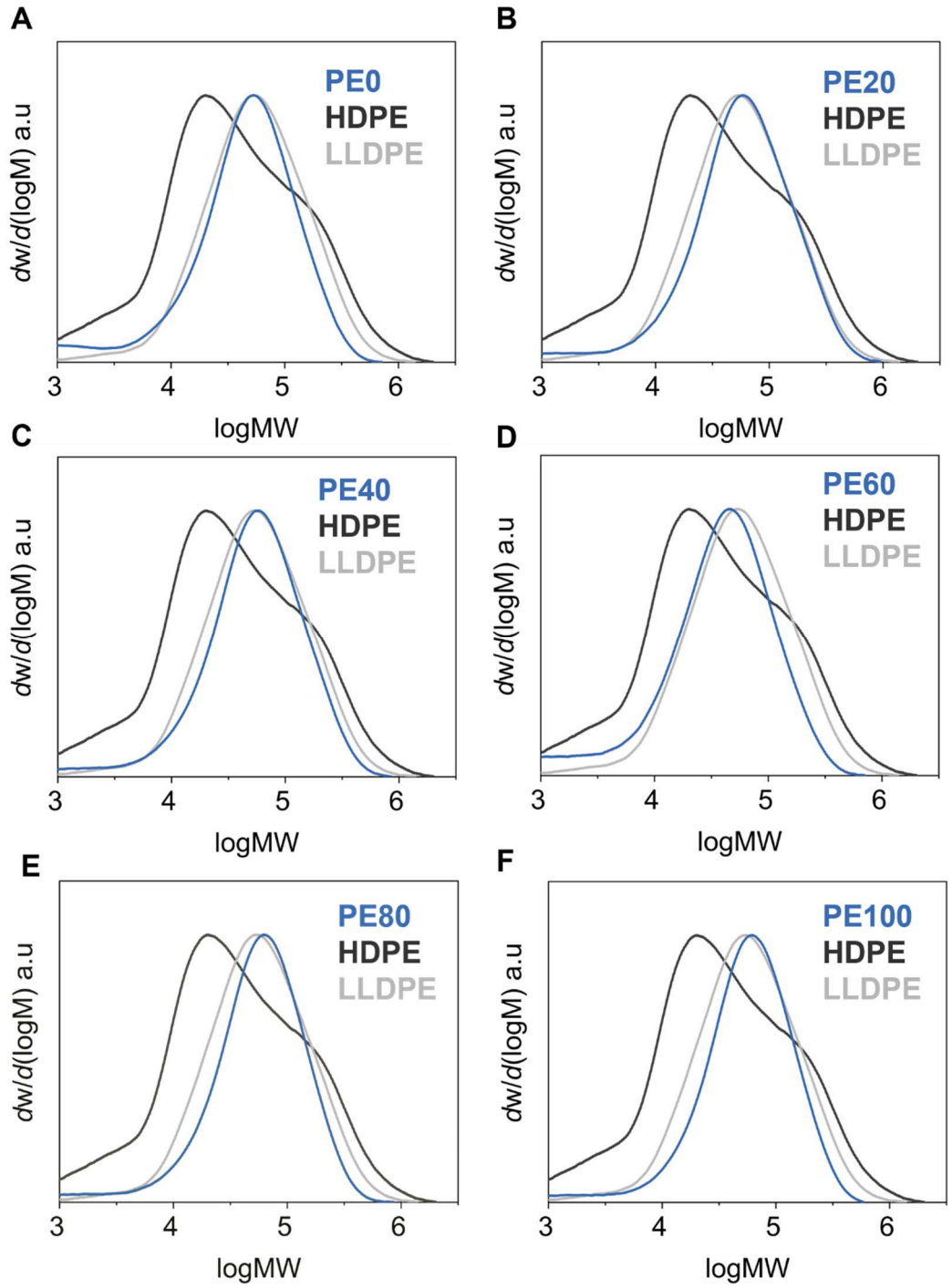


**Fig. S12.** HT-SEC traces (TCB at 160 °C) of synthesized copolymers **PE0–PE100** in comparison with HDPE and LLDPE.

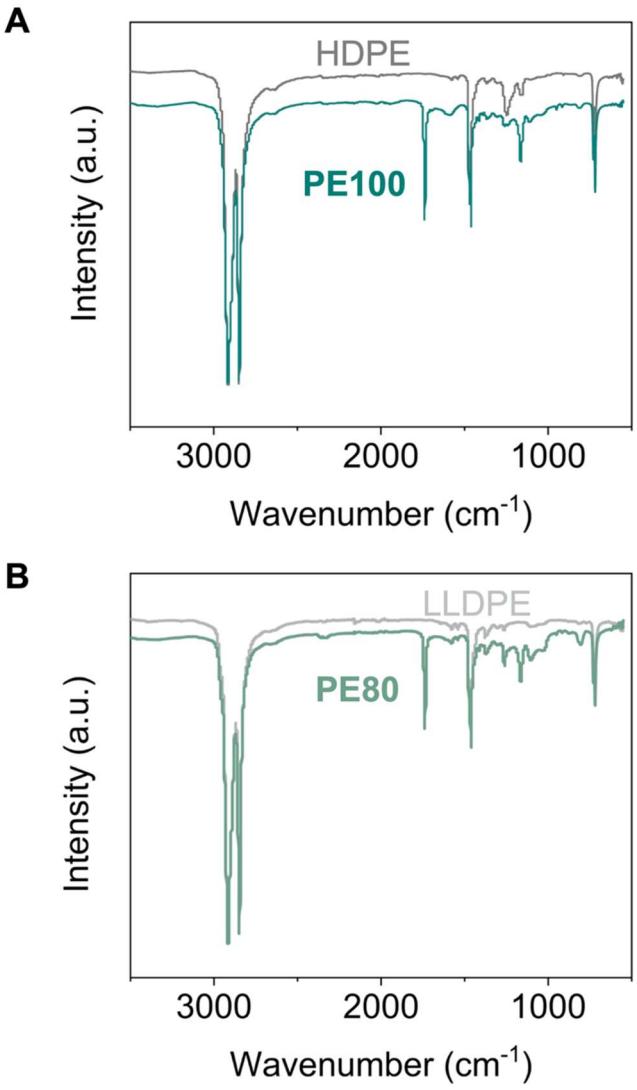


**Fig. S13.** Overlayed FT-IR spectra for (A) **PE100** and HDPE, (B) **PE80** and LLDPE.

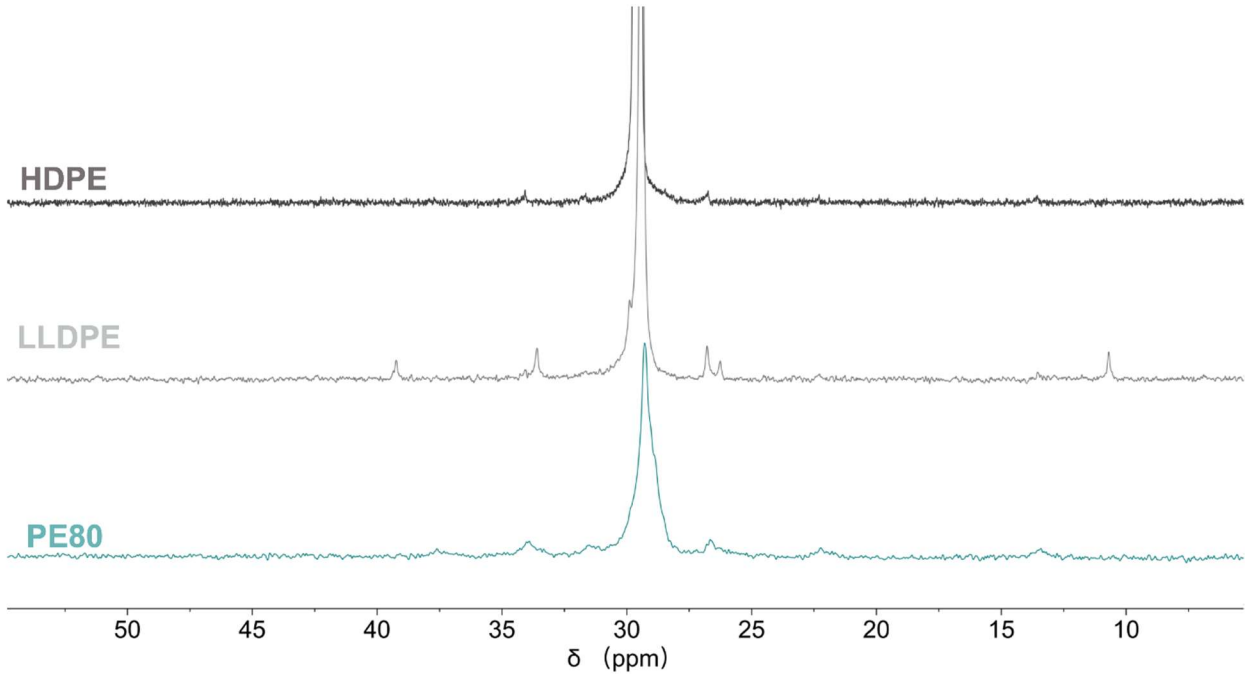


**Fig. S14.** $^{13}$C NMR spectra (403 K, 125 MHz, tetrachloroethane-d2) of HDPE, LLDPE, and **PE80**.

**Table S1.** Branching numbers for samples. [a] (*39*)

| | **PE0** | **PE20** | **PE40** | **PE60** | **PE80** | **PE100** | HDPE | LLDPE |
|---|---|---|---|---|---|---|---|---|
| C6 branching (%) | 6.2 | 5.8 | 4.3 | 3.6 | 2.5 | 0 | - | - |
| Branching number (per 1000C) | 62 | 58 | 43 | 36 | 25 | 0 | 1.9[b] | 30[c] |

[a] Branching number for PE0-PE100 was calculated based on Equation **S1**. [b]HDPE contains 0.027% methyl branches, 0.049% ethyl branches, 0.058% butyl branches and 0.063% long branches based on the $^{13}$C NMR spectroscopy of HDPE in tetrachloroethane-d2 (403 K).[c] LLDPE contains 1.70% methyl branches, 0.75% ethyl branches, and 0.53% long branches calculated based on the $^{13}$C NMR spectroscopy of LLDPE in tetrachloroethane-d2 (403 K).

**Table S2.** Composition and crystallinity data measured for copolymers and commercial polyethylene references.

| Sample | $Hard_{theo}$ | $Hard_{NMR}$ | $CO_2$ in copolymers | $M_{w,SEC}$ | $M_{n,SEC}$ | $Đ$ | Yield | $T_c$ | $\Delta H_f$ |
|---|---|---|---|---|---|---|---|---|---|
| | (mol%) | (mol%) | (per 1000C) | (kDa) | (kDa) | | (%) | (°C) | (J/g) |
| **PE0** | 0 | 0 | 4.75 | 71.7 | 26.9 | 2.4 | 94.9 | - | - |
| **PE20** | 20 | 21 | 5.74 | 90.4 | 33.4 | 2.5 | 92.5 | 72.5 | 20.0 |
| **PE40** | 40 | 46 | 6.09 | 82.4 | 31.8 | 2.4 | 91.9 | 88.3 | 47.8 |
| **PE60** | 60 | 57 | 7.66 | 62.7 | 23.0 | 2.7 | 96.3 | 96.5 | 66.0 |
| **PE80** | 80 | 76 | 8.18 | 81.0 | 33.0 | 2.5 | 92.4 | 104 | 119 |
| **PE100** | 100 | 100 | 10.4 | 80.7 | 34.0 | 2.2 | 95.9 | 109 | 191 |
| HDPE | - | - | 0 | 92.2 | 17.2 | 5.4 | - | 113 | 149 |
| LLDPE | - | - | 0 | 90.4 | 31.8 | 2.8 | - | 103 | 90.0 |
| **HO-HB-OH** | - | - | - | 3.3 | 1.9 | 1.7 | 66.3 | 113 | 260 |
| **HO-SB-OH** | - | - | - | 3.0 | 1.8 | 1.7 | 64.9 | - | - |

$Hard_{theo}$ (mol%), the theoretical molar ratio of hard blocks in copolymers. $Hard_{NMR}$ (mol%), the molar ratio of hard blocks in copolymers determined by $^1$H NMR and calculated based on Equation S2. $CO_2$ content in copolymers were calculated based on the Equation S3. $M_{n,SEC}$ (kDa), number-average molecular weight determined by HT-SEC. $M_{w,SEC}$ (kDa) weight-average molecular weight. $Đ$, molecular weight distribution. $T_c$, crystallization temperature. $\Delta H_f$, enthalpy of fusion.

Determination of residual loading of ruthenium in the copolymers and oligomers.

Polyolefin copolymers and oligomers were weighed into Teflon weighing cups and these were placed into 75 mL Teflon microwave vessels along with a blank sample. Digestion was performed by adding 9.5 mL of redistilled concentrated nitric acid (67-70% $HNO_3$). Each vessel was left to react for 15 min after which 0.5 mL of concentrated hydrochloric acid (HCl) was added to each vessel. Each vessel was left to react for 15 minutes prior to sealing to allow any pre-reactions to occur safely before being capped. Vessels were sealed with a vessel rupture disc and pressure seal and placed in a programmable Titan MPS Microwave digestion system (PerkinElmer) and samples were digested following the program in Table S9. Upon completion of the digestion, all samples were diluted with MilliQ water (18.2 MΩ) to a final volume of 50 mL. Samples were vortexed and subsequently 3 mL of sample was diluted to a final volume of 15 mL with MilliQ water. This resulted in a final sample matrix consisting of 2.5% $HNO_3$ and <1% HCl. Additionally, 3 mL of each sample was combined into a pooled QC sample.

**Table S3.** The residual content of ruthenium in the copolymers and oligomers. [a]

| sample | [Ru] (ppm) | Purification method | $[Ru]_p$ (ppm) |
|---|---|---|---|
| **PE100** | 958.3 | Precipitation, recrystallization (Method A+B) | 643.9 |
| **PE100** | 958.3 | Precipitation with ligand (Method C) | 88.99 |
| **PE100**[b] | 451.7 | Precipitation with ligand (Method C) | 413 |
| **PE60** | 1131 | Precipitation with ligand (Method C) | 598.7 |
| **PE80** | 2113 | - | - |
| **PE80 RP1** | 1546 | - | - |
| **PE80 RP2** | 1919 | - | - |
| **PE80 RP3** | 1506 | Precipitation with ligand (Method C) | 755.1 |
| **HO-HB-OH** | - | Recrystallization (Method B) | 144.1 |
| **HO-SB-OH** | - | Flash chromatography (Method D) | 1.05 |

[a] The residual loadings of ruthenium catalyst in the copolymers were determined by ICP-MS. [Ru] is the ruthenium loading in the copolymers before purification. $[Ru]_p$ is the ruthenium loading in the copolymers after purification. Ligand = 2-aminoethanethiol (0.02 $M^{-1}$ in xylene). [b] **PE100** was made using **Ru-2** as catalyst (see Table S5, entry S5).

**Table S4**. Titan MPS digestion program for digestion of polymer samples.

| Step | Target Temp (°C) | Pmax (bar) | Ramp (min) | Hold (min) | Power (%) |
|---|---|---|---|---|---|
| 1 | 170 | 30 | 5 | 5 | 90 |
| 2 | 200 | 30 | 3 | 40 | 100 |
| 3 | 50 | 30 | 1 | 15 | 0 |

Polymerization using different Pincer catalysts.

**Table S5.** Polymerization results using different Pincer catalysts.[a]

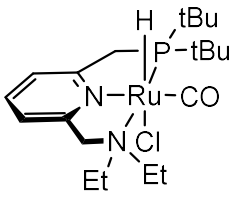


**Ru-1**

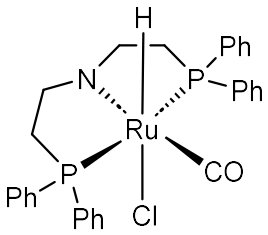


**Ru-2**

| Entry | Cat | [-OH]:[cat] | Temperature (°C) | Reaction Time (h) | $M_{w,SEC}$ (kDa) | $M_{n,SEC}$ (kDa) | $Đ$ | Yield (%) | $T_m$ (°C) | $\Delta H_f$ (J/g) | $X_c$ (%) |
|---|---|---|---|---|---|---|---|---|---|---|---|
| S1 | **Ru-1** | 100:0.5 | 150 | 48 | 54.9 | 23.3 | 2.35 | 92.4 | 124 | 151.4 | 53.7 |
| S2 | **Ru-1** | 100:0.25 | 150 | 48 | 55.0 | 23.1 | 2.39 | 94.7 | 123 | 183.1 | 65.2 |
| S3 | **Ru-1** | 100:0.125 | 150 | 48 | 6.1 | 3.8 | 1.59 | 87.5 | 127 | 222.2 | 79.1 |
| S4 | **Ru-1** | 100:0.5 | 130 | 72 | 38.1 | 18.5 | 2.06 | 91.8 | 125 | 210.0 | 74.7 |
| S5 | **Ru-2** | 100:0.5 | 130 | 48 | 92.8 | 32.3 | 2.88 | 95.1 | 124 | 174.3 | 62.0 |
| S6 | **Ru-2** | 100:0.25 | 130 | 48 | 65.9 | 25.6 | 2.58 | 93.2 | 126 | 196.9 | 70.0 |
| S7 | **Ru-2** | 100:0.125 | 130 | 72 | 68.4 | 25.8 | 2.65 | 91.6 | 126 | 188.2 | 67.0 |

[a] Conditions: 1.00 mmol **HO-HB-OH**, [-OH]:[*t*-BuOK] = 100:4, catalyst (1.00 mM in solvent). $M_{n,SEC}$ (kDa), number-average molecular weight determined by HT-SEC. $M_{w,SEC}$ (kDa) weight-average molecular weight. *Đ,* molecular weight distribution. $T_m$ is measured with DSC.

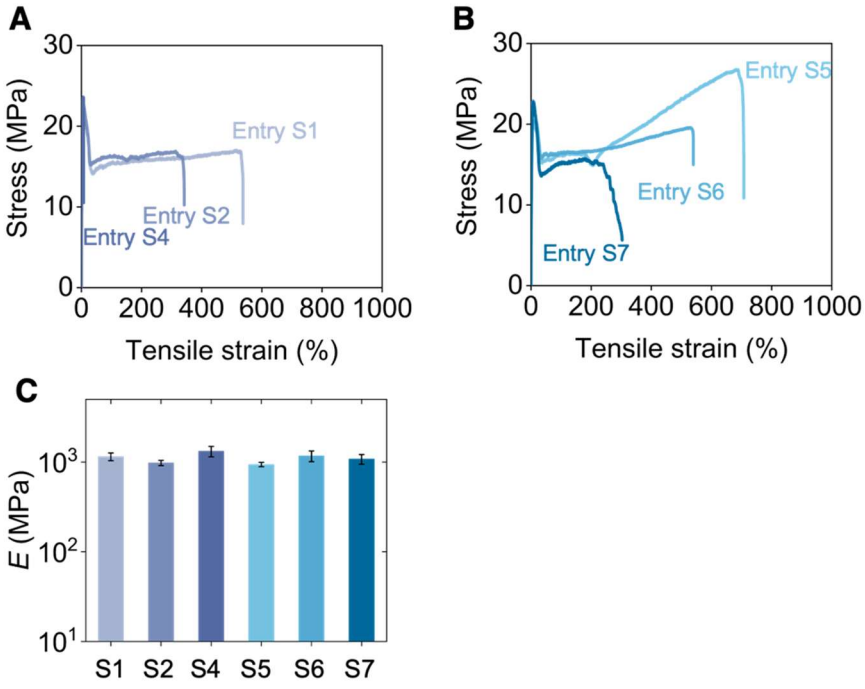


**Fig. S15.** (A) Representative stress-strain curves of **PE100** using **Ru-1** with different loadings. (The sample in entry S3 was not measured due to the low molecular weight). (B) Representative stress-strain curves of **PE100** using **Ru-2** with different loadings. (C) Young's modulus of **PE100**s for Table S5.


**Fig. S16.** Photos of **PE100** in Table S5. Sample in entry S3 was not processed due to the low molecular weight. (A) Using **Ru-1** as the catalyst. (B) Using **Ru-2** as the catalyst, pale-yellow materials were synthesized.

Thermogravimetric Analysis for copolymers, HDPE, and LLDPE.

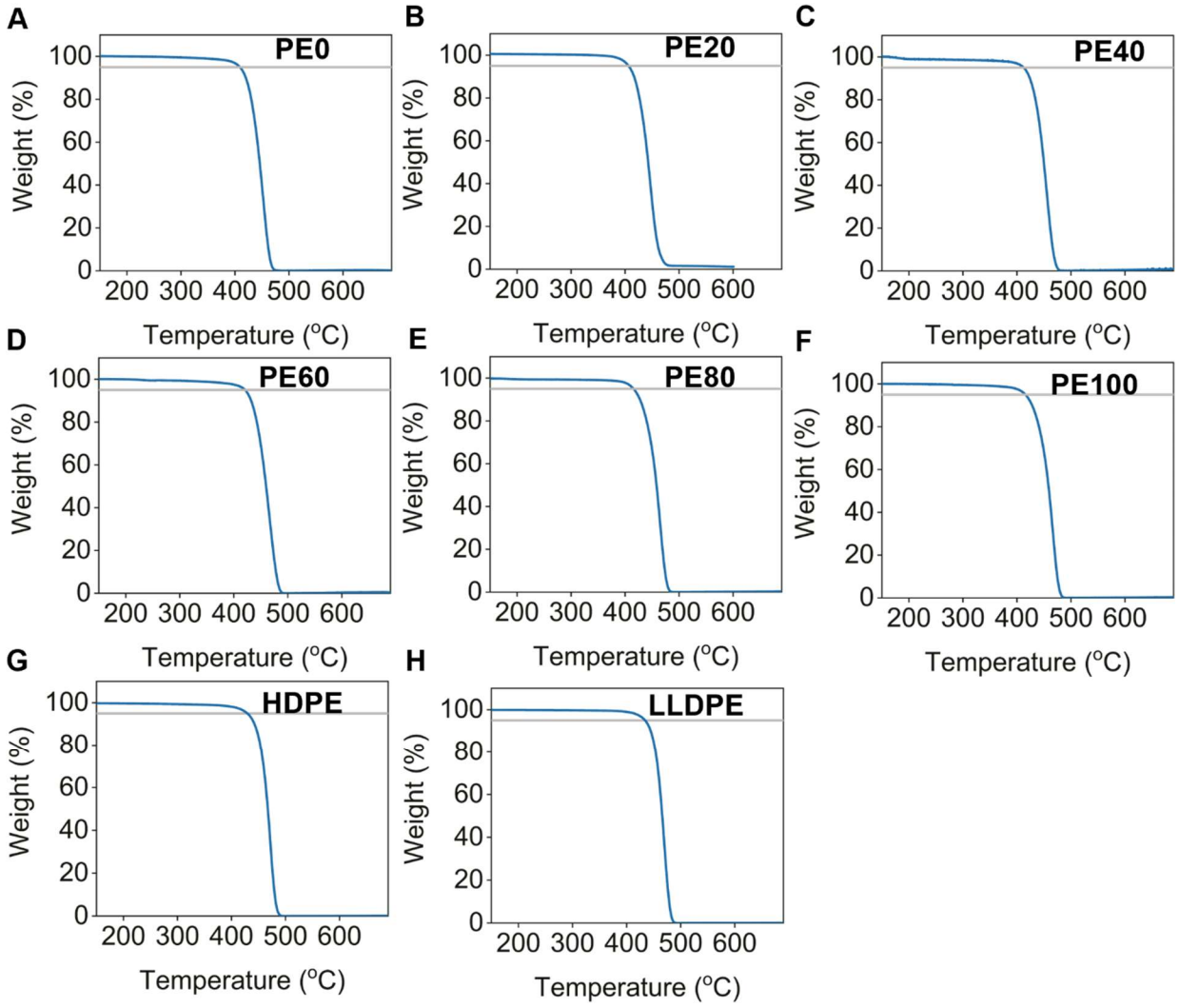


**Fig. S17.** Thermogravimetric analysis of (A) **PE0** ($T_{d5}$ = 409 °C), (B) **PE20** ($T_{d5}$ = 406 °C), (C) **PE40** ($T_{d5}$ = 413 °C), (D) **PE60** ($T_{d5}$ = 421 °C), (E) **PE80** ($T_{d5}$ = 416 °C), (F) **PE100** ($T_{d5}$ = 415 °C). which are comparable with (G) HDPE ($T_{d5}$ = 430 °C) and (H) LLDPE ($T_{d5}$ = 434 °C).

Differential Scanning Calorimetry analysis for copolymers, HDPE, and LLDPE.

*Calculation of degree of crystallinity ($X_c$) in homopolymers and copolymers:*
The crystallinity of the materials were calculated using their measured $\Delta H_f$ integrations on heating compared to the equilibrium heat of fusion for fully crystalline polyethylene (*40*) ($\Delta H_f^\circ$ = 281 J g$^{-1}$) of relevant molecular weight ($M_w$ = 60.7 kDa) according to:

$$X_c = \frac{\Delta H_f^{meas}}{\Delta H_f^\circ} \times 100\%$$

Equation **S4**

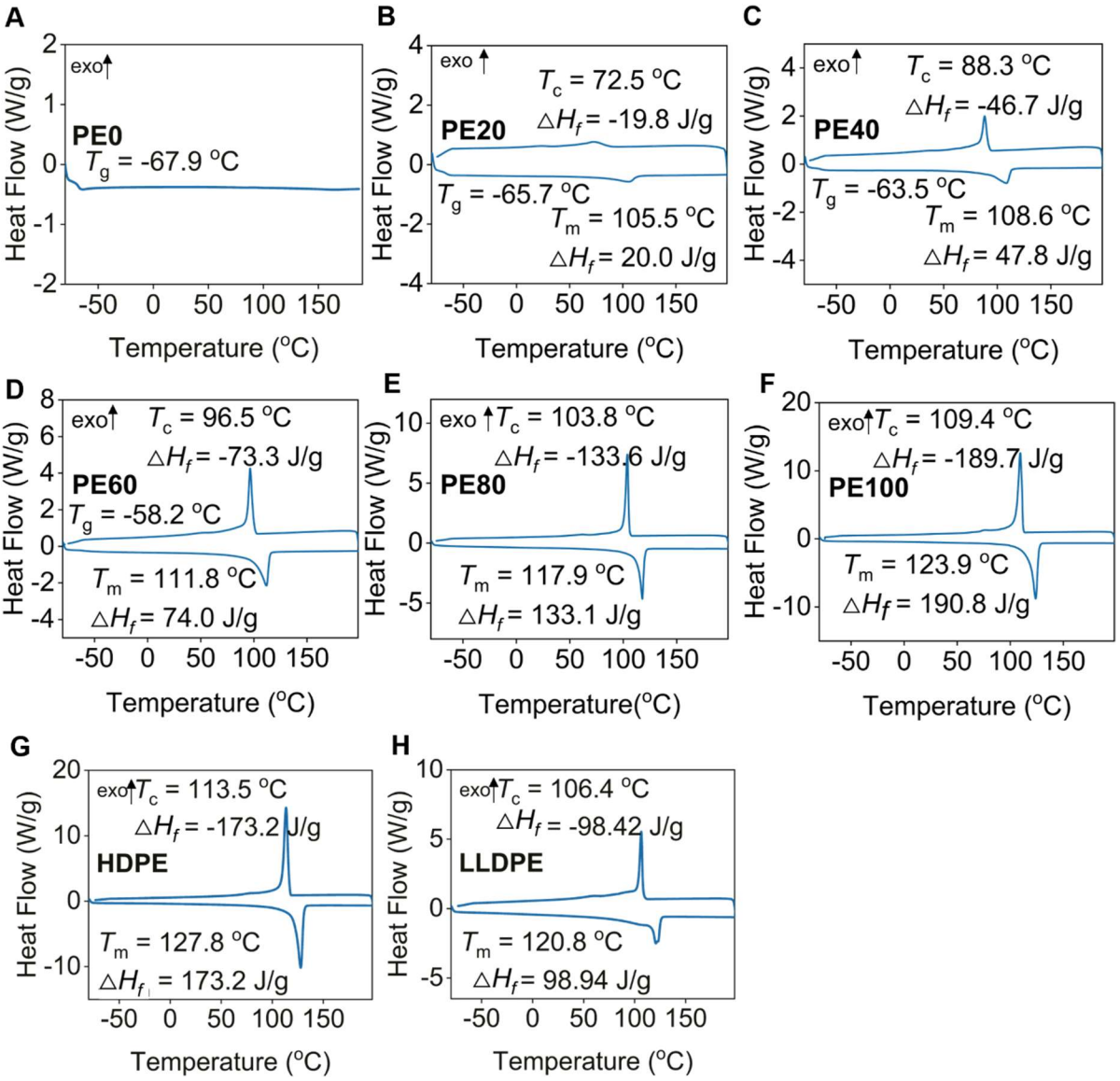


**Fig. S18**. DSC traces of **PE0–PE100**, HDPE and LLDPE, including both heating and cooling scans (scan rate = 10 °C/min). The data was collected from the second heating cycle.

Dynamic Mechanical Thermal Analysis (DMTA) analysis for copolymers, HDPE, and LLDPE.

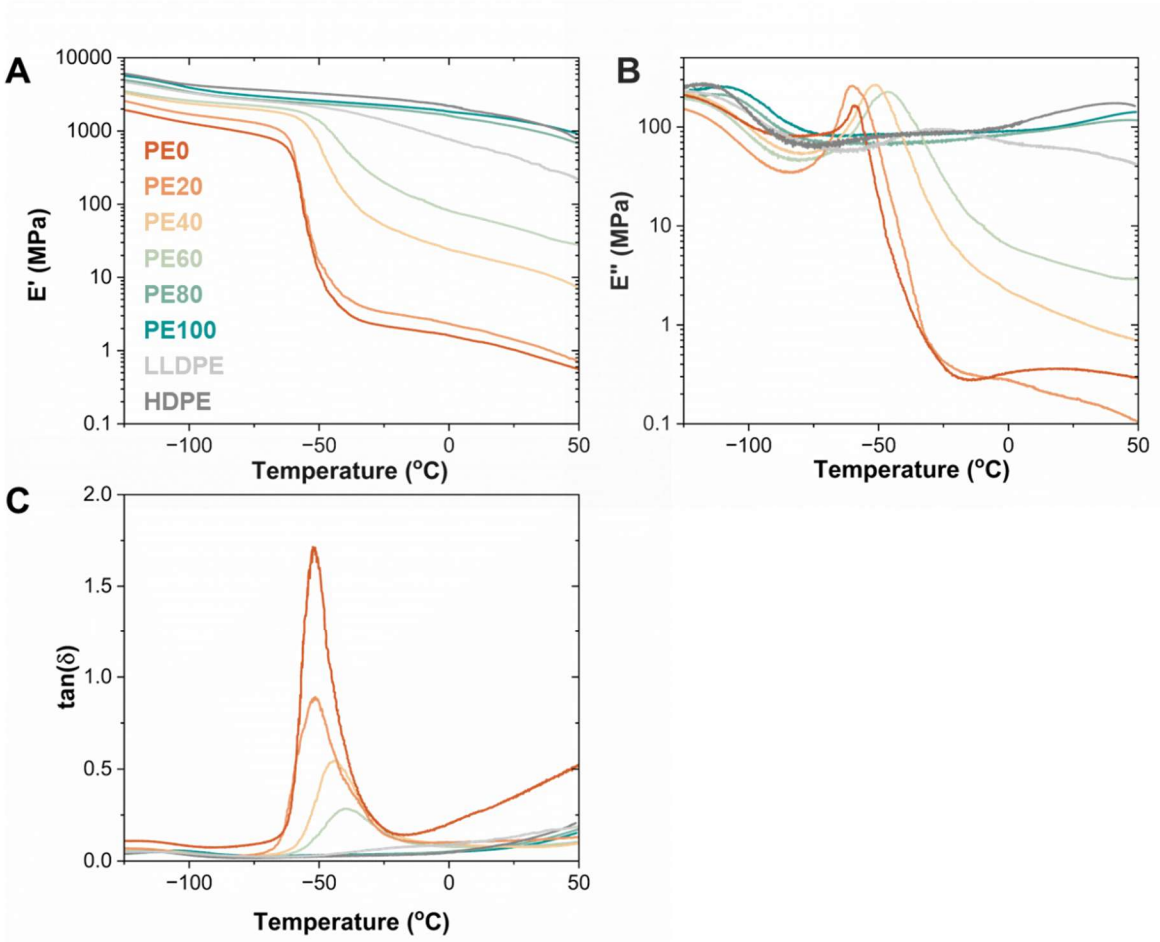


**Fig. S19.** Dynamic mechanical relaxation behavior for multiblock polymers and polyethylene controls, showing (A) Storage Modulus *E'*, (B) Loss Modulus *E"*, and tan($\delta$). $T_g$ was determined as the peak of the loss modulus *E"* and was not detected for samples **PE80, PE100**, and HDPE, consistent with high degrees of crystallinity and low amorphous content, limiting detection of the glass transition.

**Table S6.** Locations of characteristic peaks from DMTA and comparison to $T_g$ from DSC.

| | HDPE | LLDPE | **PE0** | **PE20** | **PE40** | **PE60** | **PE80** | **PE100** |
|---|---|---|---|---|---|---|---|---|
| Peak of *E*" (°C) | - | -27.4 | -59.0 | -60.0 | -50.6 | -46.5 | - | - |
| Peak of tan(δ) (°C) | - | - | -52.5 | -52.7 | -53.8 | -39.9 | - | - |
| $T_g$ (°C) from DSC | - | - | -67.9 | -65.7 | -63.5 | -58.2 | - | - |

**Table S7.** Properties of olefin copolymers, **PE0–PE100**, and commercial polyolefins.

| Sample Type | Sample | Density ($g/cm^3$) | $T_g$ (°C) | $X_c$ (%) | $T_m$ (°C) | Modulus (MPa) | $\varepsilon_b$ (%) | $\sigma_{UTS}$ (MPa) |
|---|---|---|---|---|---|---|---|---|
| Recyclable multiblock Polyolefins [a] (this work) | **PE0** | 0.876 | -59.1 | 0 | - | 0.58±0.05 | 700 ± 100 | 0.041±0.006 |
| | **PE20** | 0.876 | -60.0 | 7.1 | 106 | 5.4±0.2 | 1000±100 | 3.3±0.3 |
| | **PE40** | 0.902 | -50.6 | 17 | 109 | 15±1 | 1030±30 | 12.0±0.7 |
| | **PE60** | 0.910 | -46.5 | 26 | 112 | 84±4 | 710±40 | 23±1 |
| | **PE80** | 0.950 | - | 43 | 117 | 279±8 | 720±60 | 24±2 |
| | **PE100** | 0.966 | - | 68 | 124 | 800±30 | 720 ± 60 | 25±2 |
| Ethylene-octene olefin block copolymers (chain shuttling polymerization) | **SS** [b] | 0.858 | -44 | - | - | 3.0 | 1239 | - |
| | **H18** [b,c] | 0.865 | -43 | 7 | 114 | 5.9±0.2 | 1234±54 | - |
| | **H27** [b] | 0.880 | -42 | 17 | 118 | 18±1 | 1096±66 | - |
| | **H40** [b] | 0.893 | -34 | 27 | 119 | 43±2 | 1042±66 | - |
| | **H57** [b] | 0.902 | -31 | 31 | 121 | 72±1 | 925±36 | - |
| | **H67** [b] | 0.910 | -19 | 40 | 122 | 98±1 | 896±40 | - |
| | **H82** [b] | 0.920 | | 47 | 124 | 166±2 | 831±37 | - |
| | **HS** [b] | 0.935 | - | 57 | 126 | 275±3 | 997±53 | - |
| | **OBC** [d] | 0.883 | - | 124 | - | - | - | - |
| | **OBC** [d] | 0.883 | - | 121 | - | - | - | - |
| | **OBC** [d] | 0.879 | - | 120 | - | - | - | - |
| Ethylene-octene olefin **random** copolymers [c] | **EO87** | 0.872 | -36 | 13 | 61 | 13±1 | 748±29 | - |
| | **H7-O** | 0.918 | - | - | 113 | - | - | - |
| | **H10-O** | 0.913 | - | - | 108 | - | - | - |
| | **H16-O** | 0.900 | - | - | 94.5 | - | - | - |
| | **L4-O** | 0.937 | - | - | 119 | - | - | - |
| | **L24-O** | 0.898 | - | - | 90.2 | - | - | - |
| | **L39-O** | 0.870 | - | - | 48.2 | - | - | - |
| Dow's commercial olefin block copolymers (OBCs) [e] | **INFUSE9530** | 0.887 | -62 | - | 119 | 3.8 | 1300 | 7.4 |
| | **INFUSE9900** | 0.880 | -50 | - | 122 | 4.0 | 780 | 4.42 |
| | **INFUSE9500** | 0.877 | -62 | - | 122 | 2.3 | 1150 | 5.0 |
| | **INFUSE9077** | 0.869 | -65 | - | 118 | 1.2 | >750 | 3.0 |
| | **INFUSE9507** | 0.866 | -62 | - | 119 | 1.5 | 1210 | 2.9 |
| Dow's commercial Random copolymers [f] | **ENGAGE™8842** | 0.857 | -58 | - | 38 | 1.40 | 1200 | 3.0 |
| | **ENGAGE™8180** | 0.863 | -55 | - | 47 | 1.90 | 910 | 6.3 |
| | **ENGAGE™ 8658** | 0.902 | -36 | - | 96 | 6.70 | 910 | 11.3 |
| | **ENGAGE™8440 G** | 0.897 | -33 | - | 93 | 6.30 | 690 | 20.4 |
| | **ENGAGE™ 8669** | 0.873 | -53 | - | 76 | 2.85 | >1100 | 5.95 |
| | **ENGAGE™8540 G** | 0.908 | -32 | - | 104 | 9.60 | 750 | 27.9 |
| HDPE and LLDPE [k] | HDPE [a] | 0.948 | - | 53 | 128 | 1100±100 | 530 ±40 | 25 ±1 |
| | HDPE [g] | 0.961 | - | - | 134 | 1200 | - | 30 |

| | | | | | | | |
|---|---|---|---|---|---|---|---|
| HDPE [h] | 0.953 | - | 70 | 132 | - | >800 | 23 |
| LLDPE [a] | 0.918 | -27.4 | 32 | 121 | 270 ±10 | 750 ±60 | 28 ± 2 |
| LLDPE (octene coM) [i] | 0.920 | - | - | 116 | - | 770 | 11 |
| LLDPE [j] | 0.940 | - | - | 126 | 625 | 460 | 20.7 |

[a] Data measured in this work. Glass transition temperature ($T_g$) determined by DMTA, crystallinity ($X_c$) from DSC, Young's modulus, tensile strength ($\sigma_{UTS}$), elongation at break ($\varepsilon_b$). Densities for **PE0–PE100** prepared by melt compression at 150 °C and quenching at 30 °C/min to room temperature. [b] Data is from (*41*). Modulus value corresponds to 5% secant modulus. [c] Data is from (*42, 43*). [d] Data is from (*23*). [e] Data is from (*44*). [f] Data is from (*45*). [g] Data is from (*46*). [h] Data is from (*20*). [i] Data is from (*47*). [j] Data is from (*48*). [k] The glass transition temperatures of linear polyethylenes are generally agreed to occur between approximately -120 °C and -50 °C (*49, 50*).

Wide-angle X-ray Scattering of copolymers, HDPE, and LLDPE.

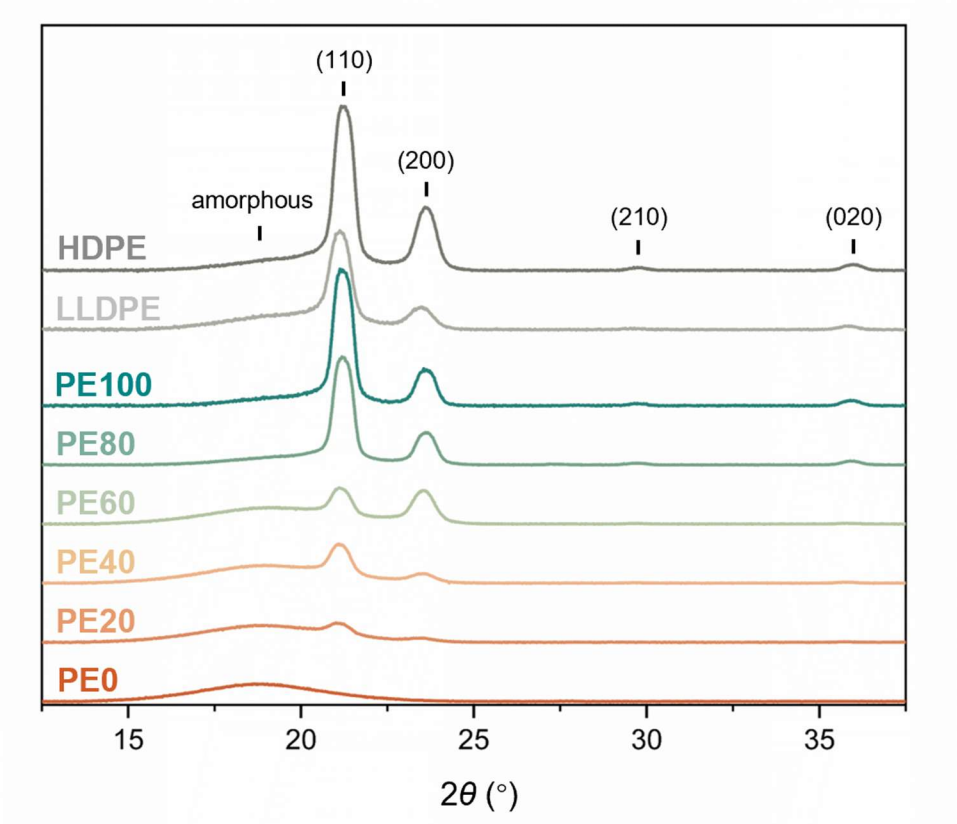


**Fig. S20**. Overlaid X-ray scattering patterns for multiblock polymers **PE0–PE100**, LLDPE and HDPE, showing contributions from the orthorhombic unit cell of polyethylene as well as amorphous polyethylene. The relative intensities of the crystalline components increase while the amorphous component decreases with increasing hard content.

Polarized Light Optical Microscopy (PLOM) of copolymers, HDPE, and LLDPE.

Crystallites are evident in all samples possessing hard blocks and can be observed to increase in size as a function of hard block content. Overall, multiblock crystallites are reduced in size compared to control polyethylene samples with no ester content (i.e., **PE100** to HDPE, **PE80** to LLDPE).

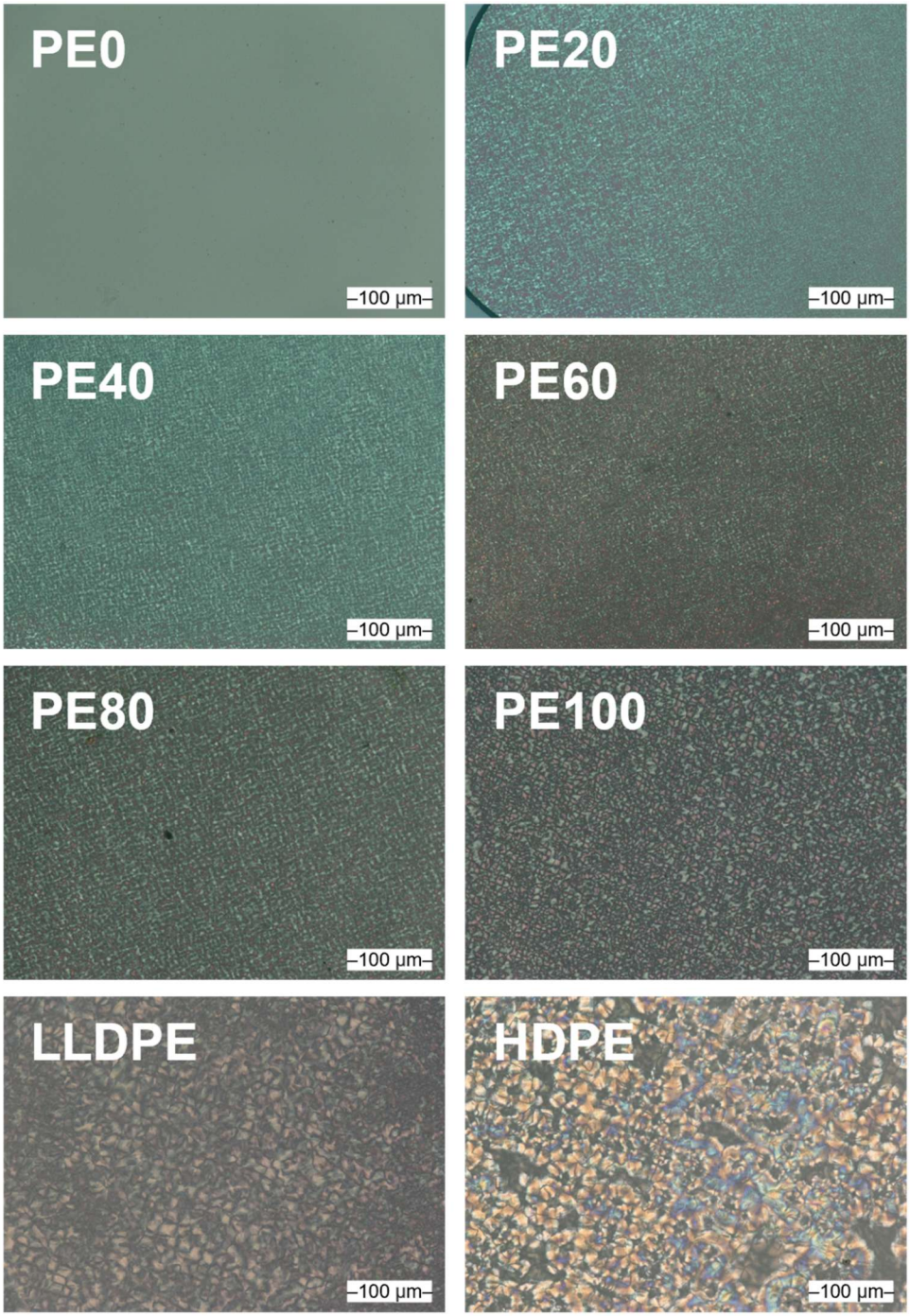


**Fig. S21.** PLOM images at 500x magnification of multiblock polymers and polyethylene controls.

Creep tests for zero-shear viscosity of copolymers, HDPE, and LLDPE.

The relationship of creep compliance of melted copolymers and step time were measured by rheology at 150 °C to determine the zero-shear viscosity of copolymers from the creep compliance $J(t')$ according to:

$$\log \eta_0 = \lim_{t' \to \infty} \left( \log \left( \frac{t'}{J} \right) \right)$$

Equation **S5**

Per equation S5, zero shear viscosity was extrapolated from these curves to the limit of zero shear. For linear PE, a direct correlation between zero shear viscosity and the molecular weight is expected.

However, our observations of non-linear relationships between zero-shear viscosity and average degree of branching are consistent with observations from the literature. Stadler et al (*30*) report that correlations between long-chain branched polyethylenes and linear polyethylenes can be made by the addition of a scaling factor, where the zero shear viscosity of the branched polyolefin is normalized by that of a linear polyethylene of the same $M_w$. Additionally, the authors discuss that architectures such as LDPE and comb-like PE do not adhere to the linear polyethylene $\eta_0$-$M_w$ relation even with this scaling factor applied. The topology of the soft blocks is consistent with comb-like architectures, and the different incorporation of these segments between **PE0–PE80** may cause zero-shear rate behavior that is between that of comb-like and linear architectures. Further explanation for the irregularity is not possible at this time, as treatment of **PE100** as this linear analogue for **PE0–PE80** would be non-exact because of the $M_w$ discrepancy between these samples.

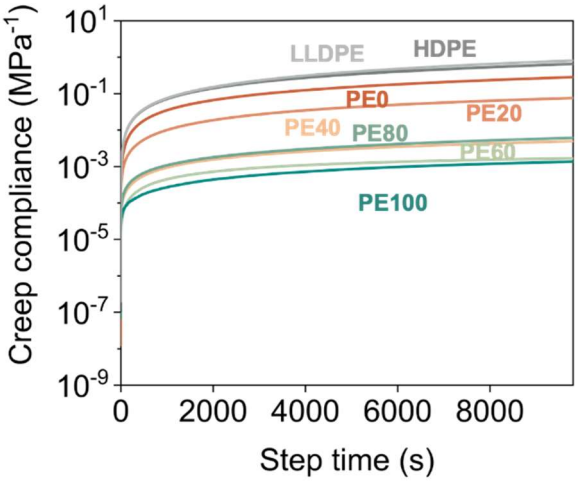


**Fig. S22.** The relationship of creep compliance with step time for **PE0–PE100**, HDPE, and LLDPE.

**Table S8.** Molecular weight data and zero shear-rate viscosities of the copolymers, HDPE, and LLDPE. [a]

| Samples | $M_w$ (kDa) | $Đ$ | Branches per 1000C | Branching type | $\eta_o$ (Pa·s) |
|---|---|---|---|---|---|
| **PE0** | 71.7 | 2.4 | 62 | C6 branching | $3.45\times10^5$ |
| **PE20** | 90.4 | 2.5 | 58 | C6 branching | $8.88\times10^5$ |
| **PE40** | 82.4 | 2.4 | 43 | C6 branching | $21.1\times10^5$ |
| **PE60** | 62.7 | 2.7 | 36 | C6 branching | $68.7\times10^5$ |
| **PE80** | 81.0 | 2.5 | 25 | C6 branching | $21.4\times10^5$ |
| **PE100** | 80.7 | 2.2 | 0 | - | $447\times10^5$ |
| HDPE | 92.2 | 5.4 | 1.9 | - | $2.47\times10^5$ |
| LLDPE | 90.4 | 2.8 | 30 | C1, C2, and long chain branching | $1.30\times10^5$ |
| HDPE [b] | 42 | 3 | - | - | 520 |
| HDPE [b] | 120 | 2 | - | - | $1.78\times10^4$ |
| HDPE [b] | 224 | 3 | - | - | $1.13\times10^5$ |
| HDPE [b] | 563 | 4.3 | - | - | $67.3\times10^5$ |
| mHDPE [b] | 106 | 2.5 | 3.6[c] | C6 branching | $>10^8$ |
| mHDPE [b] | 240 | 2.1 | 0.27[c] | C6 branching | $12\times10^5$ |
| mLLDPE[b] | 94 | 2.2 | 1.2[c] | C6 branching | $4.2\times10^4$ |
| LLDPE[b] | 94 | 2.2 | 0.28[c] | C6 branching | $4.2\times10^4$ |
| LLDPE[b] | 190 | 2.0 | 0.20[c] | C6 branching | $4.4\times10^5$ |
| LLDPE[b] | 240 | 2.1 | 1.2[c] | C6 branching | $12\times10^5$ |
| OBC-R01[d] | 122 | 2.4 | 58 | C6 branching | $3.39\times10^4$ |
| OBC-R03[d] | 156 | 2.2 | 83 | C6 branching | $6.82\times10^5$ |
| OBC-R09[d] | 136 | 2.1 | 70 | C6 branching | $13.65\times10^5$ |
| OBC-R17[d] | 124 | 2.1 | 60 | C6 branching | $3.94\times10^4$ |
| EO1[e] | 94.5 | 2.4 | 25 | C6 branching | $4.2\times10^4$ |
| EO2[e] | 106 | 2.5 | 37.5 | C6 branching | $3.5\times10^4$ |
| EO3[e] | 121 | 2.3 | 47.5 | C6 branching | $3.25\times10^4$ |

[a] Zero shear viscosity (Pa·s) was determined by creep testing at 150 °C. Branches per 1000 C were determined by $^1$H and $^{13}$C NMR. [b] Data is from (*30*). mHDPE = metallocene-HDPE, mLLDPE = metallocene-LLDPE. [c] Data is converted from monomer ratio in copolymers. [d] Data is from (*51*). Zero shear viscosity (Pa·s) was tested at 135 °C. [e] Ethylene-octene random copolymers. Data is from (*52*).

Uniaxial tensile testing of copolymers, HDPE, and LLDPE.

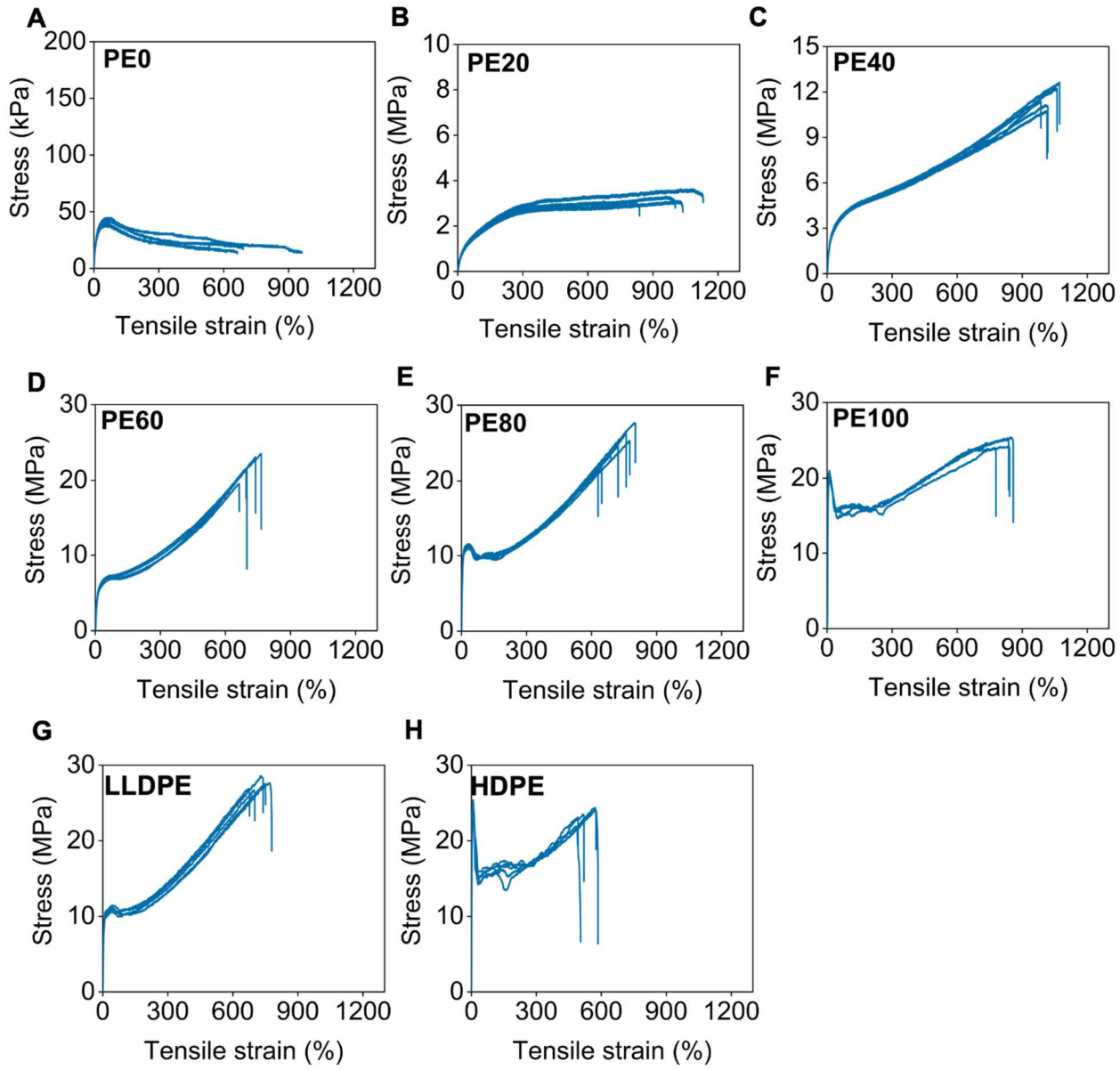


**Fig. S23.** Tensile stress-strain curves for samples **PE0–PE100**, LLDPE and HDPE. Material toughness of these samples were calculated by manual integration of the area under the tensile curve. The Young's modulus ($E$), tensile strength ($\sigma_{UTS}$), elongation at break ($\varepsilon_b$) and toughness ($U_T$) were determined based on the stress-strain curves as presented in **Table 1**.

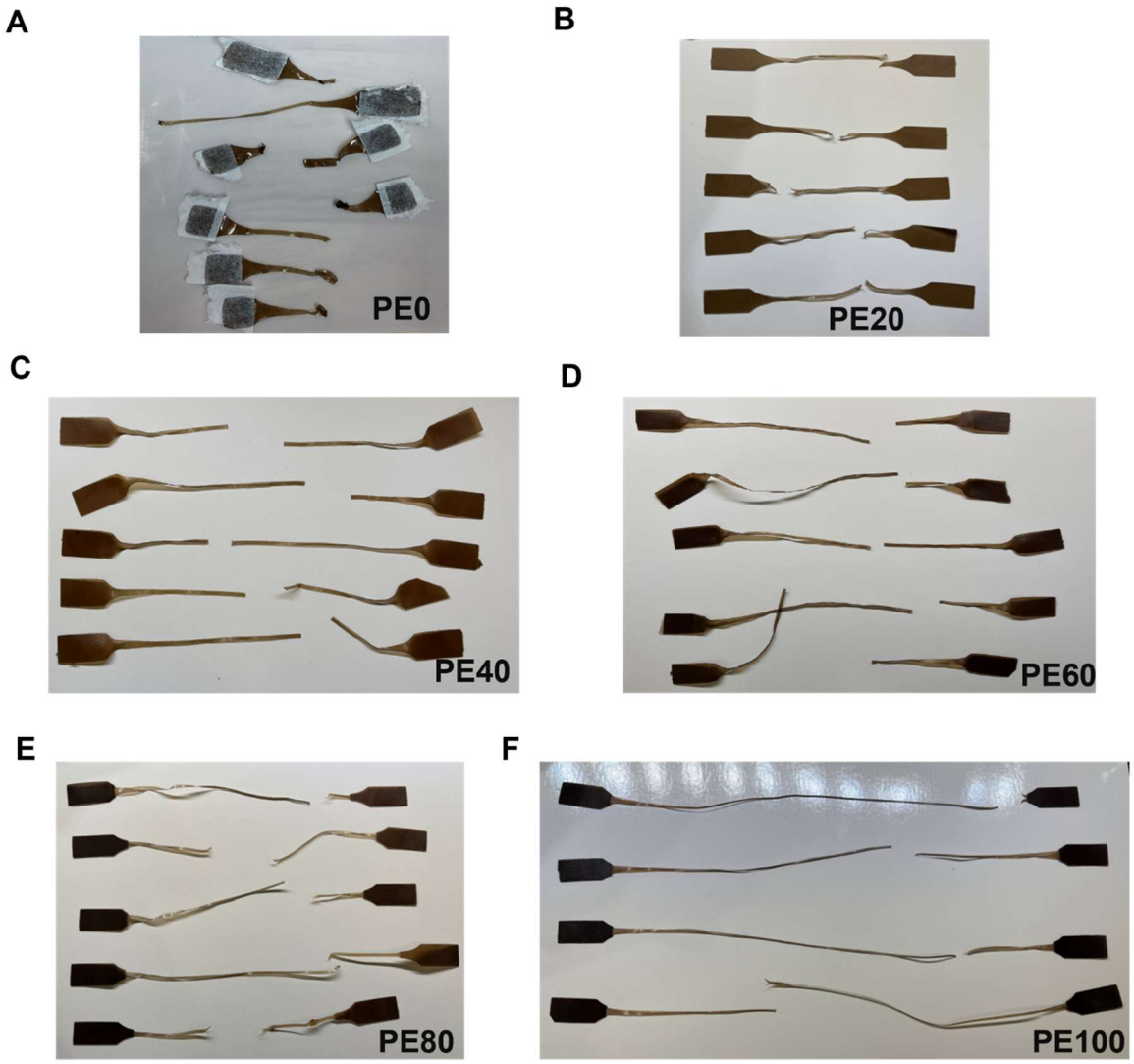


**Fig. S24.** Photographs of PE samples after tensile testing.

Mechanical properties of **PE0–PE100**, olefin block copolymers (OBCs), and random copolymers.

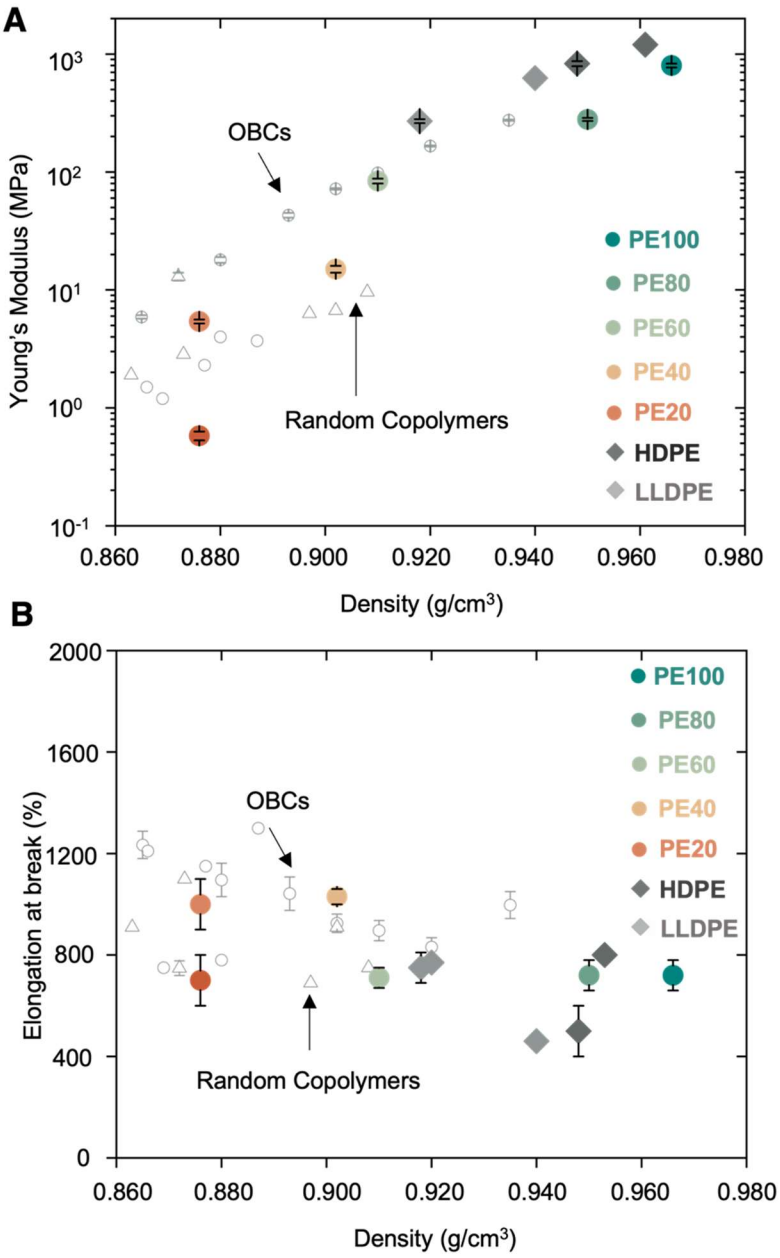


**Fig. S25.** (A) Young's modulus (*E*) of copolymers as a function of density. (B) Elongation at break of copolymers as a function of density. Data of copolymers and OBC is from Table S7 (ref (*23*), *(41), (43) and (44)*). Data of random copolymer is from EO87 and Dow's commercial random copolymers (Table S7) (ref (*20), (41), (42), (45) ~ (48)*).

Instrumentation and setup for depolymerization experiments.

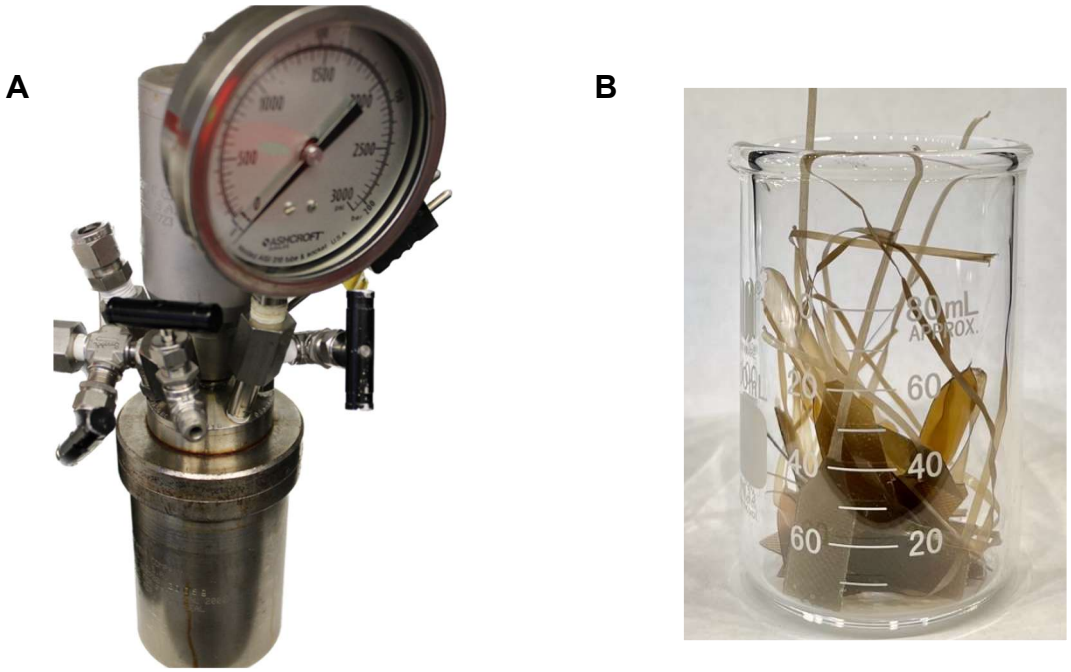


**Fig. S26.** Photographs of (A) the autoclave used for depolymerization and (B) glass beaker as an inlet with polymers for depolymerization.

Optimization of depolymerization.

The depolymerization of the multiblock copolymers using Pincer catalysts was investigated using different reaction conditions. To depolymerize the samples back to oligomers, the catalyst, solvents, temperatures, reaction pressure, and reaction time were optimized using PE0 for screening.

**Table S9.** Optimization for depolymerization of **PE0**[a]

| Entry | [ester]:[cat]:[*t*-BuOK] | Temperature (°C) | Solvent | Pressure (bar) | Reaction time (h) | Conversion (%)[b] |
|---|---|---|---|---|---|---|
| S8 | 100:1:1 | 130 | anisole | 20 | 24 | 0 |
| S9 | 100:1:1 | 130 | anisole | 40 | 24 | 0 |
| S10 | 100:1:1 | 130 | anisole | 60 | 24 | 0 |
| S11 | 100:1:1 | 130 | anisole | 40 | 48 | 0 |
| S12 | 100:5:5 | 130 | anisole | 40 | 48 | 0 |
| S13 | 100:2.5:10 | 130 | anisole | 40 | 48 | 26 |
| S14 | 100:2.5:50 | 130 | anisole | 40 | 48 | 85 |
| S15 | 100:2.5:50 | 150 | anisole | 40 | 72 | 87 |
| S16 | 100:2.5:50 | 150 | THF/anisole[c] | 40 | 72 | 95 |
| S17 | 100:2.5:50 | 150 | toluene | 40 | 72 | 99 |
| S18 | 100:2.5:50 | 150 | toluene | 40 | 48 | 90 |
| S19 | 100:1:50 | 150 | toluene | 40 | 48 | 97 |
| S20 | 100:1:50 | 160 | toluene | 40 | 24 | 99 |
| S21 | 100:1:50 | 175 | toluene | 40 | 24 | 99 |
| S22 | 100:0:50 | 160 | toluene | 40 | 24 | 99 |
| S23[d] | 100:1:50 | 160 | toluene | 40 | 24 | 99 |
| S24[e] | 100:0.5:50 | 160 | toluene | 40 | 24 | 96 |

[a] Conditions: 0.02 mmol **PE0**, **Ru-1** (2.22 mM in solvent).

[b] Conversions were determined by $^{1}$H NMR in tetrachloroethane-d2 (383 K) by analyzing the integration of ester bonds before and after reactions.

[c] THF/anisole = 1:1 by volume.

[d] **Ru-2** was used.

[e] PE100 was used after removing the catalyst (89 ppm Ru in polymer)

Depolymerization of mixed PE copolymers.

In a $N_2$ filled glovebox, 907 mg **PE0**, 949 mg **PE20**, 980 mg **PE40**, 1.03 g **PE60**, 1.01 g **PE80**, and 1.03 g **PE100** (5.91 g PE copolymers in total) were combined in a 100 mL beaker with a stir bar. 161 mg potassium *t*-butoxide (0.500 eq of the ester bond) and 35.0 mL toluene solution of **Ru-1** (1.00 mg/mL, 2.50 mol% to the ester bond) were used for depolymerization. The mixture was combined in an autoclave and reacted with 40 bar $H_2$ at 150 °C for 72 h. After cooling to room temperature and degassing the conversion was determined by $^1$H NMR as 100% (Fig. S27). The mixture was separated and purified to give 3.08 g hard blocks and 2.34 g soft blocks (91.7% total isolated yield).

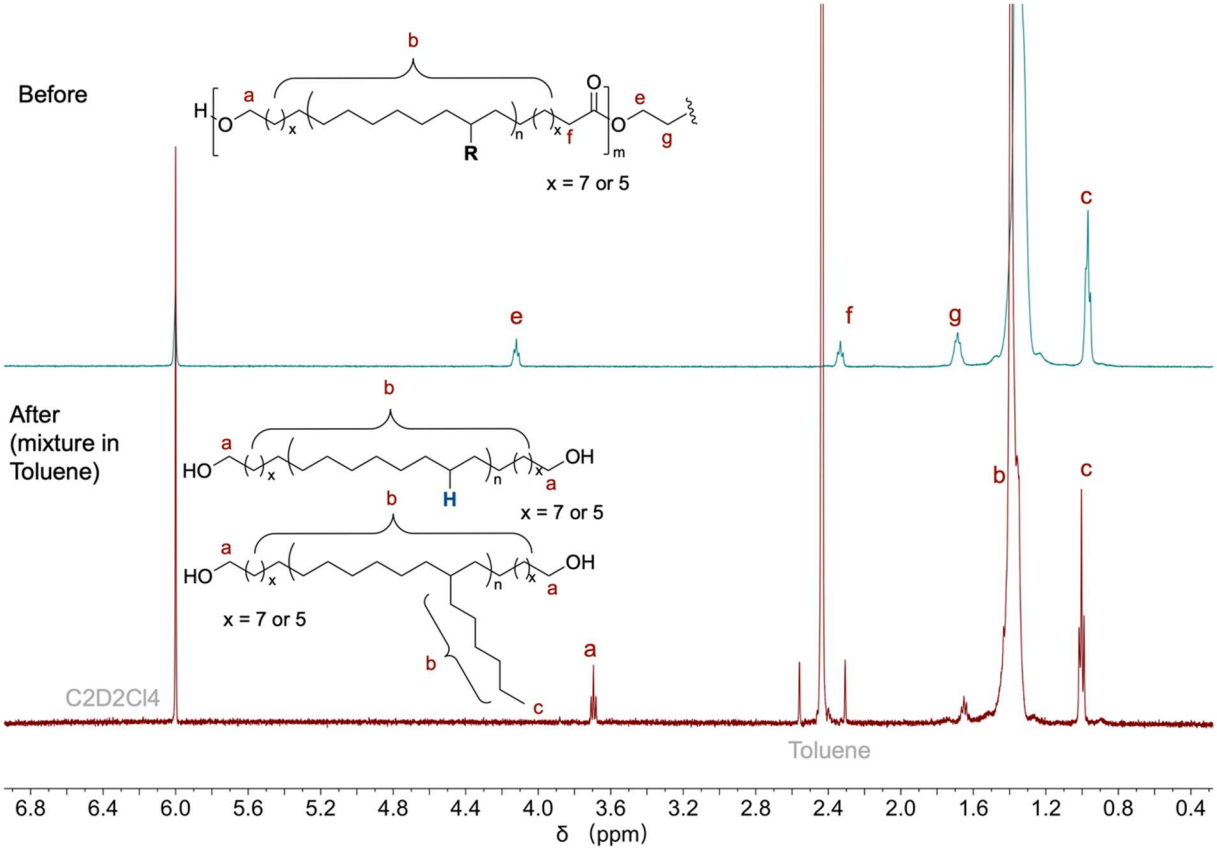


**Fig. S27.** $^1$H NMR spectra (383 K, 500 MHz, tetrachloroethane-d2) of mixed copolymers and recycled oligomers (mixture in toluene).

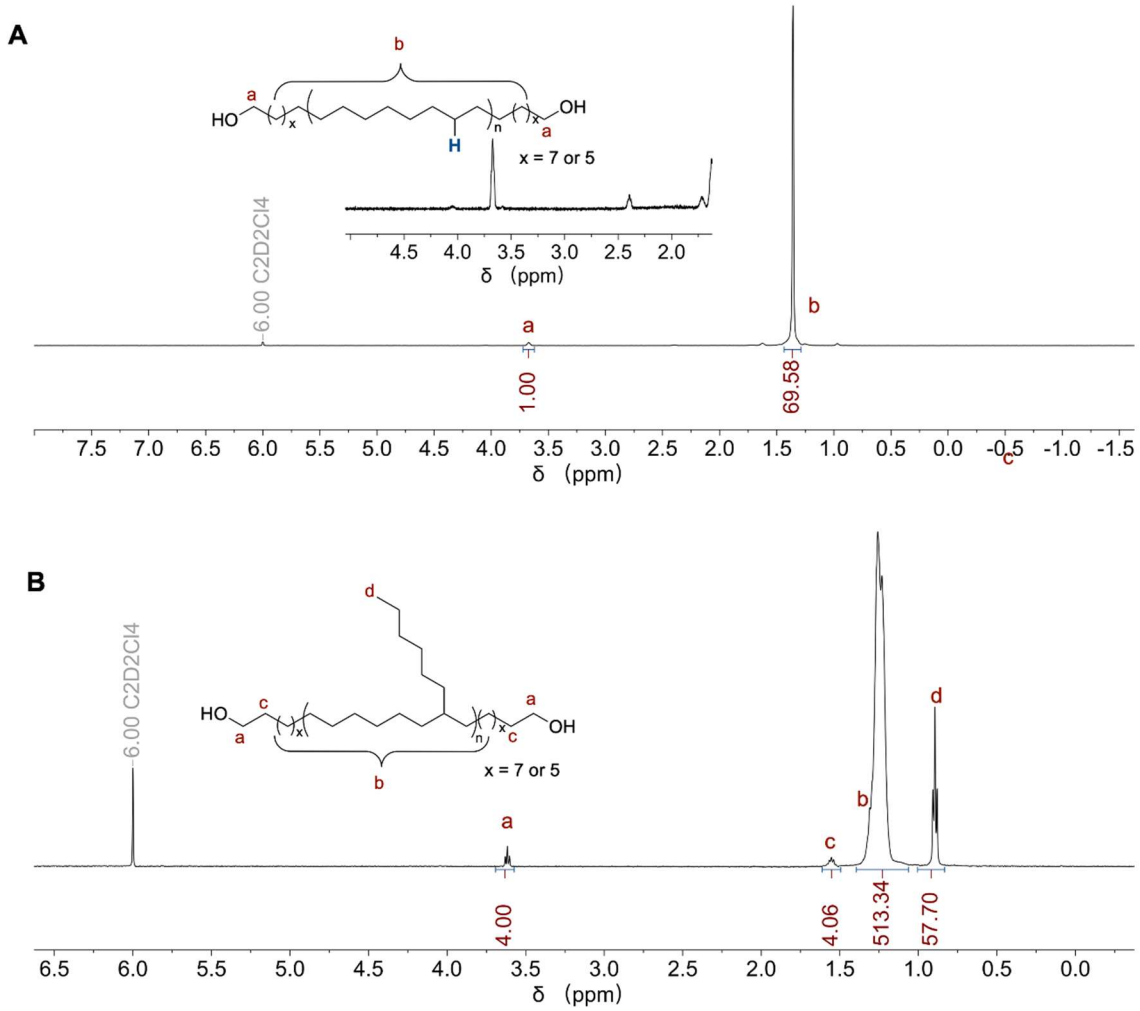


**Fig. S28**. $^{1}$H NMR spectra (500 MHz, tetrachloroethane-d2) of recycled and purified oligomers. (A) Recycled hard blocks (383 K). (B) Recycled soft blocks (298 K).

Recycling of **PE80**.

2.52 g **OH-HB-OH** and 1.10 g **OH-SB-OH** from the depolymerization of mixed copolymers were dried in a 50 mL Schlenk tube at 130 °C under vacuum for 2 h. Under $N_2$ flow, a 20.0 mL anisole solution of **Ru-1** (1.00 mg/mL, 1.00% to the -OH bond) was added to the storage tube via syringe, and the temperature was raised to 150 °C with stirring. The mixture was stirred for 48 h. Then, the mixture was diluted with 25.0 mL xylene at 140 °C, precipitated in isopropanol (150 mL) to give repolymerized **PE80-RP1**. The isolated **PE80-RP1** was dried under vacuum at 130 °C for 24 h.

After analysis by HT-SEC, DSC, TGA, and tensile testing, **PE80-RP1** was depolymerized back to the oligomers using the general procedure described above. Hard blocks were purified by recrystallization and soft blocks were purified by flash chromatography (THF as eluting solvent). The obtained oligomers were used to make new **PE80**.

Recycling of **PE80** was carried out three times. The corresponding data is presented in Tables S10 and S11.

**Table S10.** Data for recycled **PE80** multiblock copolymers. [a]

| Sample | Hard/soft block (g) | $M_{w,SEC}$ (kDa) | $M_{n,SEC}$ (kDa) | $Đ$ | Product (g) | Yield (%) | $T_m$ (°C) | $\Delta H_f$ (J/g) | $T_{d5}$ (°C) |
|---|---|---|---|---|---|---|---|---|---|
| **PE80** | 1.26/0.55 | 81.0 | 33.0 | 2.5 | 1.65 | 91.1 | 117 | 133.1 | 416 |
| **PE80-RP1** | 2.52/1.10 | 73.8 | 30.0 | 2.5 | 3.36 | 92.8 | 117 | 103.1 | 409 |
| **PE80-RP2** | 2.00/0.87 | 82.4 | 31.9 | 2.6 | 2.72 | 96.6 | 117 | 126.4 | 420 |
| **PE80-RP3** | 1.72/0.74 | 96.6 | 34.3 | 2.8 | 2.26 | 91.8 | 117 | 99.98 | 420 |

[a] Molecular weights and molecular weight distributions were determined by HT-SEC using TCB as solvent at 160 °C. DSC and TGA data are from Fig. S29.

**Table S11.** Data for depolymerized oligomers.

| Sample | Hard block (g) | Soft block (g) | Isolated yield (%) |
|---|---|---|---|
| PE80-DP1 | 2.06 | 0.91 | 88.4 |
| PE80-DP2 | 1.72 | 0.74 | 90.4 |

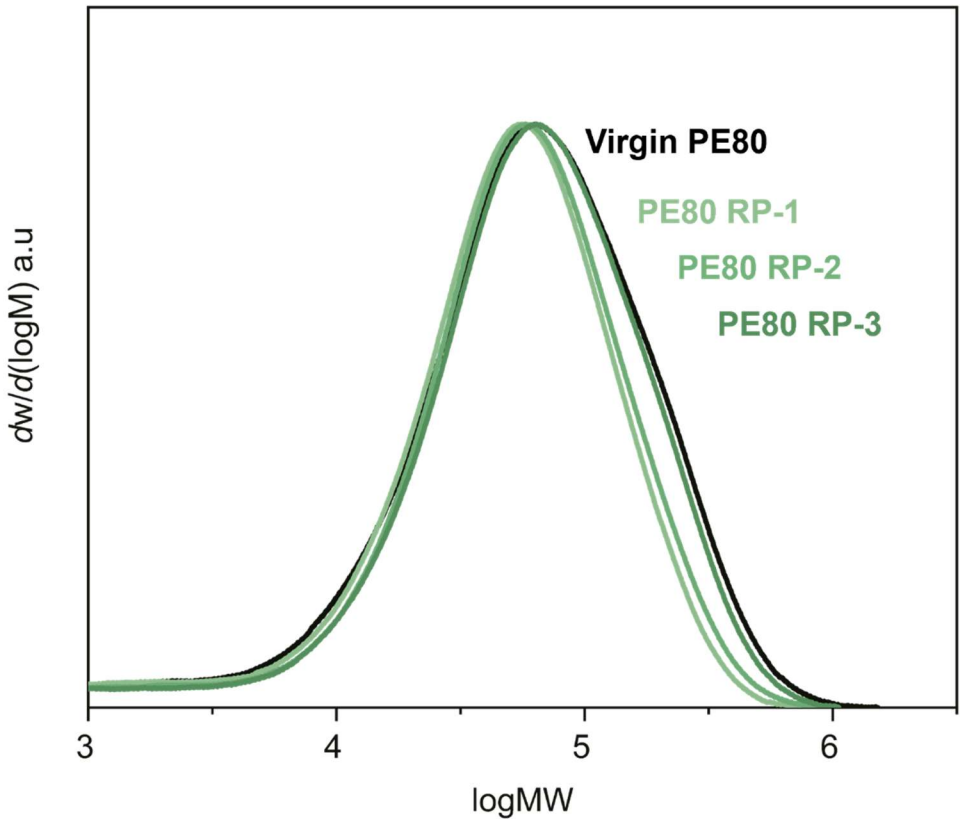


**Fig. S29.** Overlaid HT-SEC traces of the virgin **PE80**, repolymerized 1x (**PE80 RP-1**), repolymerized 2x (**PE80 RP-2**), and repolymerized 3x (**PE80 RP-3**). After complete depolymerization and repolymerization, the attainable molecular weight of chemically recycled copolymers was similar compared to the virgin polymer.

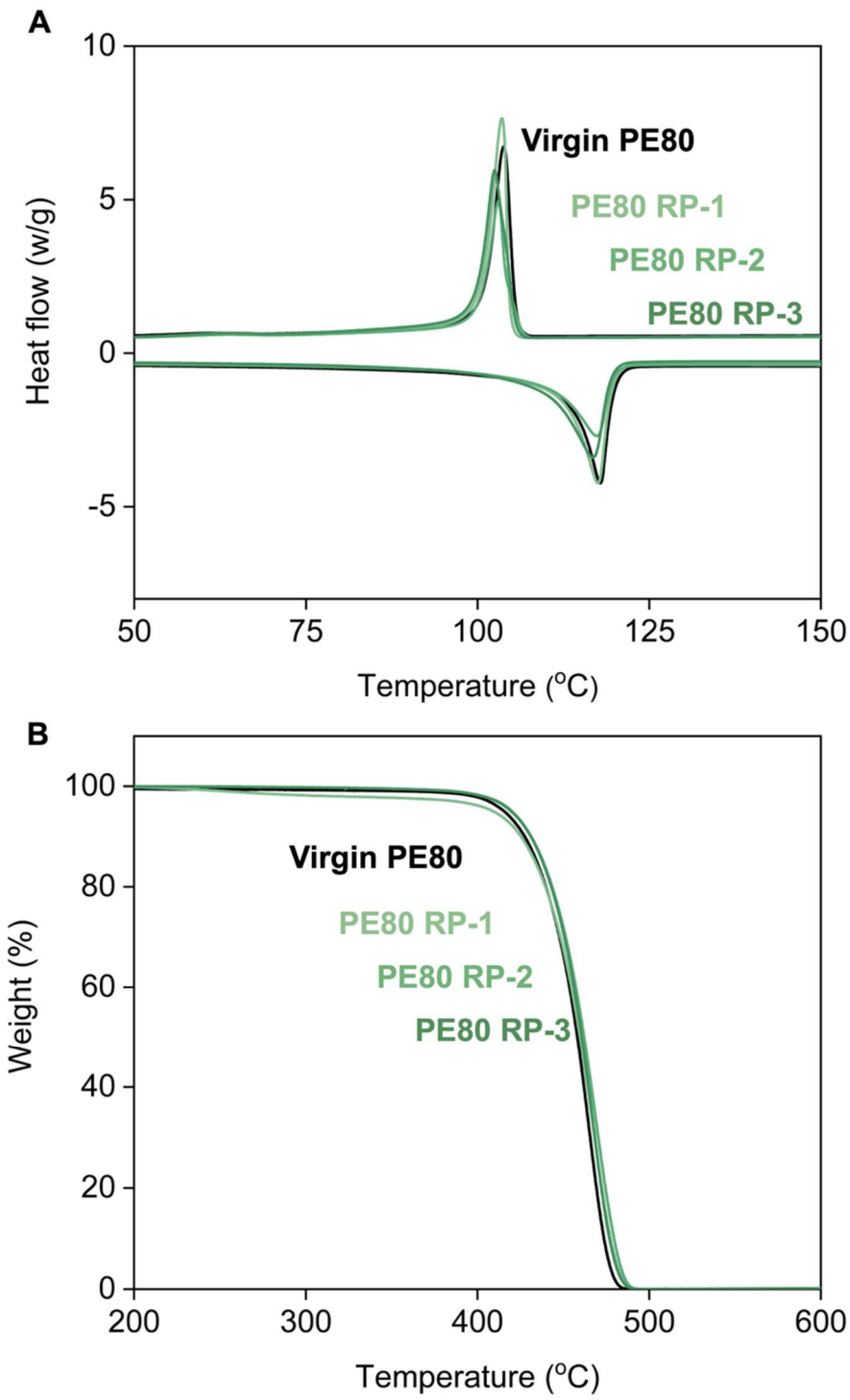


**Fig. S30.** (A) DSC traces of virgin **PE80**, repolymerized 1x (**PE80 RP-1**), repolymerized 2x (**PE80 RP-2**), and repolymerized 3x (**PE80 RP-3**). (B) TGA traces of virgin **PE80**, repolymerized 1x (**PE80 RP-1**), repolymerized 2x (**PE80 RP-2**), and repolymerized 3x (**PE80 RP-3**).

Tensile testing of recycled PE80.

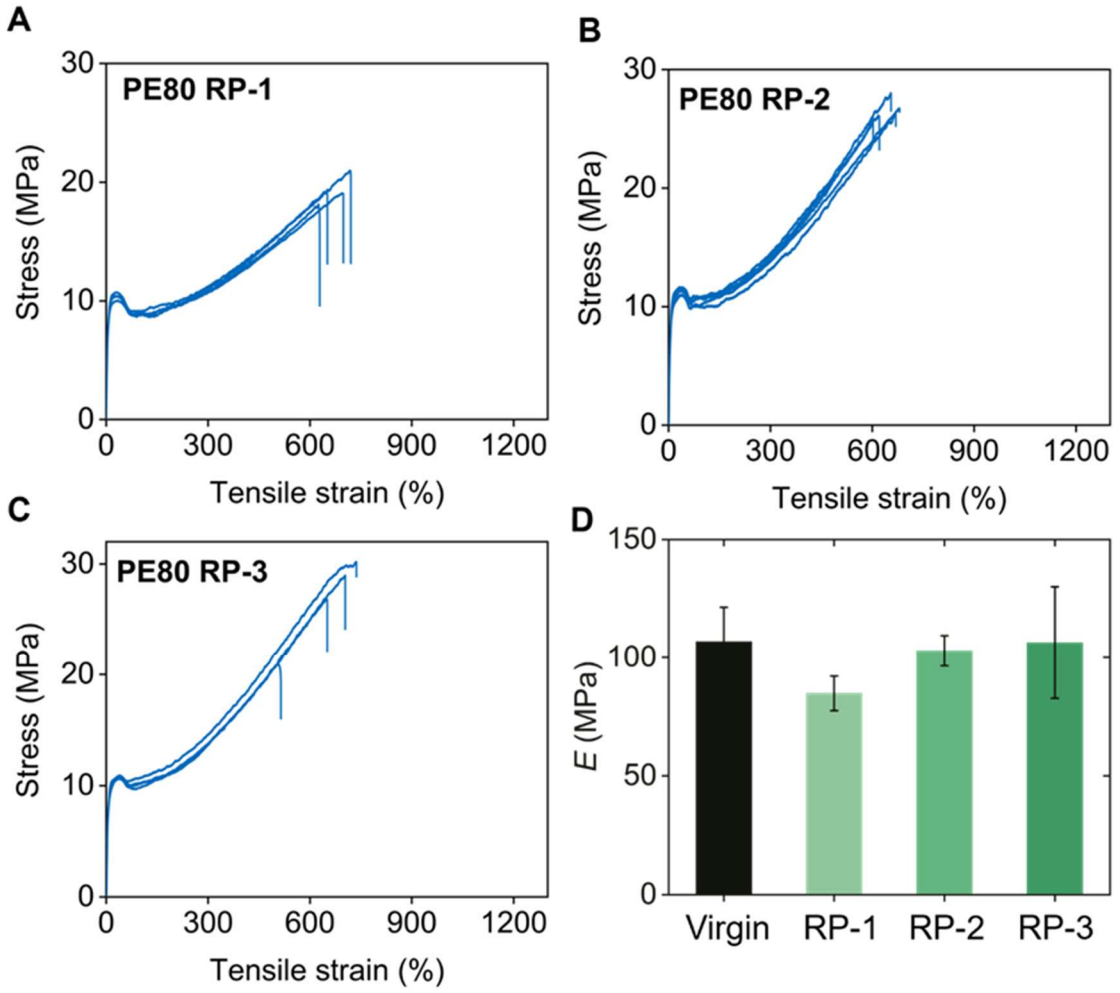


**Fig. S31.** Tensile testing of recycled (A) **PE80 RP-1**, (B) **PE80 RP-2**, and (C) **PE80 RP-3**. (D) Comparison of moduli for virgin and recycled **PE80** samples.

Depolymerization of **PE60** in the presence of polypropylene at 150 °C.

In a $N_2$ filled glovebox, 0.432 g **PE60** and a polypropylene (PP) microcentrifuge tube (0.604 g) were combined in a 25 mL vial with a stir bar. 16.3 mg potassium *t*-butoxide and 7.50 mL toluene solution of **Ru-1** (1.00 mg/mL) were added to the vial. The vial was taken out of glovebox and transferred to the pressure reactor. The reactor was sealed and cycled 4 times with 20 bar $H_2$, and then charged with 40 bar $H_2$. Then, the reactor was heated to 150 °C for 72 h. After cooling to room temperature, the reactor was depressurized, and the chamber flushed with nitrogen. A small aliquot was taken to determine conversion of **PE60** to oligomers by $^1$H NMR (>99%). The mixture was heated to 100 °C to dissolve the oligomers. After separating undissolved PP from the mixture, the solution was cooled to room temperature. Excess hexanes was added and the mixture was stirred for 30 minutes, then centrifuged to separate the solid and the solution. The solid was recrystallized in toluene to give 0.215 g hard blocks (97.7% isolated yield). The corresponding solutions and supernatant were combined and concentrated. The residue was purified by flash chromatography (eluting with THF) on silica gel to give 0.183 g soft blocks (92.0% isolated yield).

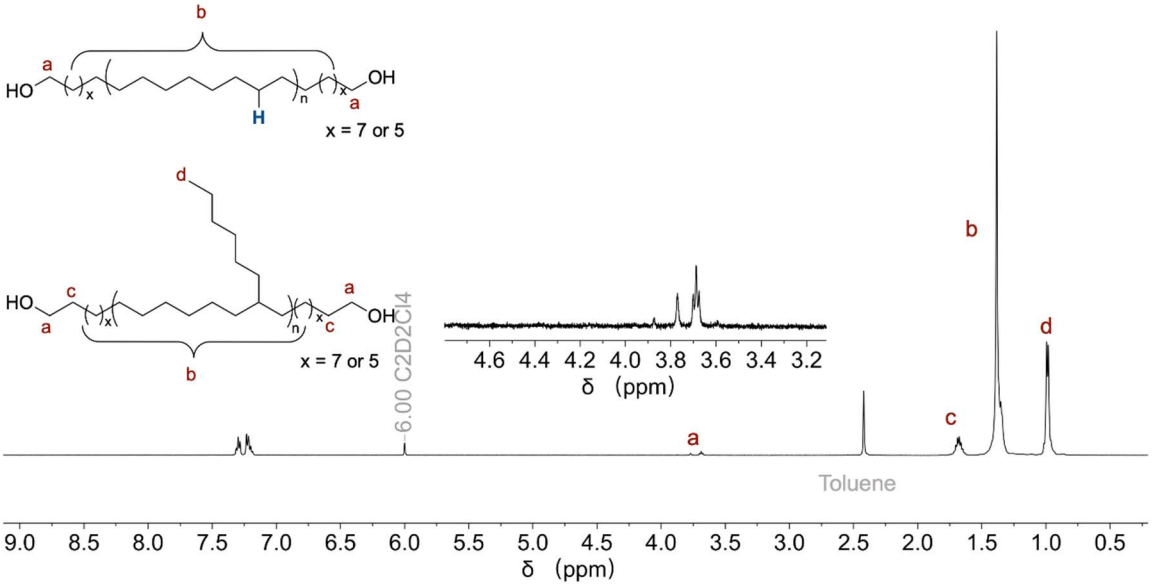


**Fig. S32.** $^1$H NMR spectra (500 MHz, tetrachloroethane-d2, 383 K) of oligomer solution (toluene) after depolymerization for 72 h.

Depolymerization of **PE60** in the presence of polypropylene at 175 °C.

*Depolymerization:* In a $N_2$ filled glovebox, 0.642 g **PE60** and a polypropylene (PP) microcentrifuge tube (0.997 g) were combined in a 25 mL vial with a stir bar. 24.2 mg potassium *t*-butoxide and 11.30 mL toluene solution of **Ru-1** (1.00 mg/mL) were added to the vial. The vial was taken out of glovebox and transferred to the pressure reactor. The reactor was sealed and cycled 4 times with 20 bar $H_2$, and then charged with 40 bar $H_2$. Then, the reactor was heated to 175 °C ($T_{m,\,PP}$ = 165 °C, and a melt blend of **PE60**/PP was formed at this temperature) for 24 h. After cooling to room temperature, the reactor was depressurized, and the chamber flushed with nitrogen. A small aliquot was taken to determine conversion of **PE60** to oligomers by $^1$H NMR (>99%).

*Separation:* The mixture was heated to 90 °C for 1 h to dissolve the oligomers. After separating undissolved solid from the mixture, the solution was cooled to room temperature. Excess hexanes was added and the mixture was stirred for 30 minutes, then centrifuged to separate the solid and the solution. The solid was recrystallized in a 10.0 mL toluene solution of 2-aminoethanethiol (0.02 $M^{-1}$), washed with isopropanol (3 × 5.0 mL), and dried under vacuum at 80 °C for 24 h to give 0.285 g hard blocks (**HO-HB-OH**, 87.2% isolated yield). The corresponding solutions and supernatant were combined and concentrated. The residue was purified by flash chromatography (eluting with THF) on silica gel to give 0.253 g soft blocks (**HO-SB-OH** 86.1% isolated yield). The former undissolved solid was dissolved in 50 mL xylene at 140 °C and recrystallized at 80 °C three times to give separated PP (0.865 g, 86.8% isolated yield).

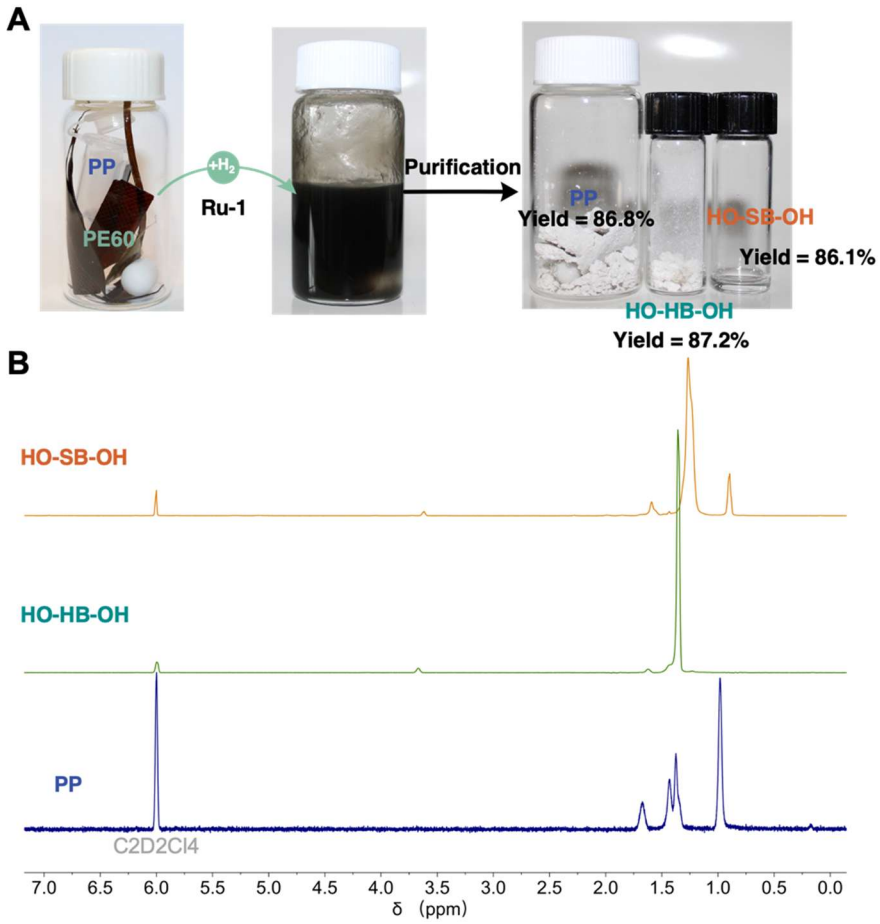


**Fig. S33.** (A) Photos of depolymerization of PP/**PE60** at 175 °C for 24 h, separated and purified oligomers, PP. (B) $^{1}$H NMR spectra (500 MHz, tetrachloroethane-d2) of purified **HO-SB-OH** (298 K), **HO-HB-OH** (383 K), and PP (403 K).

**References and Notes**


1. R. Geyer, J. R. Jambeck, K. L. Law, Production, use, and fate of all plastics ever made. *Sci. Adv.* **3**, e1700782 (2017). doi:10.1126/sciadv.1700782 Medline

2. P. Galli, G. Vecellio, Polyolefins: The most promising large-volume materials for the 21st century. *J. Polym. Sci. A Polym. Chem.* **42**, 396–415 (2004). doi:10.1002/pola.10804

3. A. Chamas, H. Moon, J. Zheng, Y. Qiu, T. Tabassum, J. H. Jang, M. Abu-Omar, S. L. Scott, S. Suh, Degradation rates of plastics in the environment. *ACS Sustain. Chem.& Eng.* **8**, 3494–3511 (2020). doi:10.1021/acssuschemeng.9b06635

4. M. MacLeod, H. P. H. Arp, M. B. Tekman, A. Jahnke, The global threat from plastic pollution. *Science* **373**, 61–65 (2021). doi:10.1126/science.abg5433 Medline

5. B. D. Vogt, K. K. Stokes, S. K. Kumar, Why is recycling postconsumer plastics so challenging? *ACS Appl. Polym. Mater.* **3**, 4325–4346 (2021). doi:10.1021/acsapm.1c00648

6. H. Li, H. A. Aguirre-Villegas, R. D. Allen, X. Bai, C. H. Benson, G. T. Beckham, S. L. Bradshaw, J. L. Brown, R. C. Brown, V. S. Cecon, J. B. Curley, G. W. Curtzwiler, S. Dong, S. Gaddameedi, J. E. García, I. Hermans, M. S. Kim, J. Ma, L. O. Mark, M. Mavrikakis, O. O. Olafasakin, T. A. Osswald, K. G. Papanikolaou, H. Radhakrishnan, M. A. Sanchez Castillo, K. L. Sánchez-Rivera, K. N. Tumu, R. C. Van Lehn, K. L. Vorst, M. M. Wright, J. Wu, V. M. Zavala, P. Zhou, G. W. Huber, Expanding plastics recycling technologies: Chemical aspects, technology status, and challenges. *Green Chem.* **24**, 8899–9002 (2022). doi:10.1039/D2GC02588D

7. R. J. Conk, S. Hanna, J. X. Shi, J. Yang, N. R. Ciccia, L. Qi, B. J. Bloomer, S. Heuvel, T. Wills, J. Su, A. T. Bell, J. F. Hartwig, Catalytic deconstruction of waste polyethylene with ethylene to form propylene. *Science* **377**, 1561–1566 (2022). doi:10.1126/science.add1088 Medline

8. F. Zhang, M. Zeng, R. D. Yappert, J. Sun, Y.-H. Lee, A. M. LaPointe, B. Peters, M. M. Abu-Omar, S. L. Scott, Polyethylene upcycling to long-chain alkylaromatics by tandem hydrogenolysis/aromatization. *Science* **370**, 437–441 (2020). doi:10.1126/science.abc5441 Medline

9. S. Liu, P. A. Kots, B. C. Vance, A. Danielson, D. G. Vlachos, Plastic waste to fuels by hydrocracking at mild conditions. *Sci. Adv.* **7**, eabf8283 (2021). doi:10.1126/sciadv.abf8283 Medline

10. X. Jia, C. Qin, T. Friedberger, Z. Guan, Z. Huang, Efficient and selective degradation of polyethylenes into liquid fuels and waxes under mild conditions. *Sci. Adv.* **2**, e1501591 (2016). doi:10.1126/sciadv.1501591 Medline

11. A. H. Mason, A. Motta, A. Das, Q. Ma, M. J. Bedzyk, Y. Kratish, T. J. Marks, Rapid atom-efficient polyolefin plastics hydrogenolysis mediated by a well-defined single-site electrophilic/cationic organo-zirconium catalyst. *Nat. Commun.* **13**, 7187 (2022). doi:10.1038/s41467-022-34707-6 Medline

12. J.-B. Zhu, E. M. Watson, J. Tang, E. Y.-X. Chen, A synthetic polymer system with repeatable chemical recyclability. *Science* **360**, 398–403 (2018). doi:10.1126/science.aar5498 Medline

13. G. W. Coates, Y. D. Y. L. Getzler, Chemical recycling to monomer for an ideal, circular polymer economy. *Nat. Rev. Mater.* **5**, 501–516 (2020). doi:10.1038/s41578-020-0190-4

14. C. Shi, L. T. Reilly, V. S. P. Kumar, M. W. Coile, S. R. Nicholson, L. J. Broadbelt, G. T. Beckham, E. Y.-X. Chen, Design principles for intrinsically circular polymers with tunable properties. *Chem* **7**, 2896–2912 (2021). doi:10.1016/j.chempr.2021.10.004

15. S. Kakadellis, G. Rosetto, Achieving a circular bioeconomy for plastics. *Science* **373**, 49–50 (2021). doi:10.1126/science.abj3476 Medline

16. F. Stempfle, P. Ortmann, S. Mecking, Long-chain aliphatic polymers to bridge the gap between semicrystalline polyolefins and traditional polycondensates. *Chem. Rev.* **116**, 4597–4641 (2016). doi:10.1021/acs.chemrev.5b00705 Medline

17. T. Shiono, N. Naga, K. Soga, Synthesis of recyclable polyolefins from α,ω-dihydroxypolybutadiene using condensation and hydrogenation reactions. *Makromol. Chem., Rapid. Commun.* **12**, 387–392 (1991). doi:10.1002/marc.1991.030120702

18. M. Baur, F. Lin, T. O. Morgen, L. Odenwald, S. Mecking, Polyethylene materials with in-chain ketones from nonalternating catalytic copolymerization. *Science* **374**, 604–607 (2021). doi:10.1126/science.abi8183 Medline

19. M. Haeussler, M. Eck, D. Rothauer, S. Mecking, Closed-loop recycling of polyethylene-like materials. *Nature* **590**, 423–427 (2021). doi:10.1038/s41586-020-03149-9 Medline

20. M. P. F. Pepels, M. R. Hansen, H. Goossens, R. Duchateau, From polyethylene to polyester: Influence of ester groups on the physical properties. *Macromolecules* **46**, 7668–7677 (2013). doi:10.1021/ma401403x

21. A. S. Arrington, J. R. Brown, M. S. Win, K. I. Winey, T. E. Long, Melt polycondensation of carboxytelechelic polyethylene for the design of degradable segmented copolyester polyolefins. *Polym. Chem.* **13**, 3116–3125 (2022). doi:10.1039/D2PY00394E

22. J. K. Stille, Step-growth polymerization. *J. Chem. Educ.* **58**, 862–866 (1981). doi:10.1021/ed058p862

23. D. J. Arriola, E. M. Carnahan, P. D. Hustad, R. L. Kuhlman, T. T. Wenzel, Catalytic production of olefin block copolymers via chain shuttling polymerization. *Science* **312**, 714–719 (2006). doi:10.1126/science.1125268 Medline

24. D. M. Hunsicker, B. C. Dauphinais, S. P. Mc Ilrath, N. J. Robertson, Synthesis of high molecular weight polyesters via in vacuo dehydrogenation polymerization of diols. *Macromol. Rapid Commun.* **33**, 232–236 (2012). doi:10.1002/marc.201100653 Medline

25. E. M. Krall, T. W. Klein, R. J. Andersen, A. J. Nett, R. W. Glasgow, D. S. Reader, B. C. Dauphinais, S. P. Mc Ilrath, A. A. Fischer, M. J. Carney, D. J. Hudson, N. J. Robertson, A. J. Nett, R. W. Glasgow, D. S. Reader, B. C. Dauphinais, S. P. McIlrath, A. A. Fischer, M. J. Carney, D. J. Hudson, N. J. Robertson, Controlled hydrogenative depolymerization of polyesters and polycarbonates catalyzed by ruthenium (II) PNN pincer complexes. *Chem. Commun.* **50**, 4884–4887 (2014). doi:10.1039/c4cc00541d

26. S. Westhues, J. Idel, J. Klankermayer, Molecular catalyst systems as key enablers for tailored polyesters and polycarbonate recycling concepts. *Sci. Adv.* **4**, eaat9669 (2018). doi:10.1126/sciadv.aat9669 Medline

27. G. W. Crabtree, M. S. Dresselhaus, M. V. Buchanan, The Hydrogen Economy. *Phys. Today* **57**, 39–44 (2004). doi:10.1063/1.1878333

28. S. Hilf, A. F. M. Kilbinger, Functional end groups for polymers prepared using ring-opening metathesis polymerization. *Nat. Chem.* **1**, 537–546 (2009). doi:10.1038/nchem.347 Medline

29. M. Gahleitner, Melt rheology of polyolefins. *Prog. Polym. Sci.* **26**, 895–944 (2001). doi:10.1016/S0079-6700(01)00011-9

30. F. J. Stadler, V. Karimkhani, Correlations between the characteristic rheological quantities and molecular structure of long-chain branched metallocene catalyzed polyethylenes. *Macromolecules* **44**, 5401–5413 (2011). doi:10.1021/ma200550c

31. T. W. Walker, N. Frelka, Z. Shen, A. K. Chew, J. Banick, S. Grey, M. S. Kim, J. A. Dumesic, R. C. Van Lehn, G. W. Huber, Recycling of multilayer plastic packaging materials by solvent-targeted recovery and precipitation. *Sci. Adv.* **6**, eaba7599 (2020). doi:10.1126/sciadv.aba7599 Medline

32. J. M. Eagan, J. Xu, R. Di Girolamo, C. M. Thurber, C. W. Macosko, A. M. LaPointe, F. S. Bates, G. W. Coates, Combining polyethylene and polypropylene: Enhanced performance with PE/*i*PP multiblock polymers. *Science* **355**, 814–816 (2017). doi:10.1126/science.aah5744 Medline

33. F. S. Bates, M. A. Hillmyer, T. P. Lodge, C. M. Bates, K. T. Delaney, G. H. Fredrickson, Multiblock polymers: Panacea or Pandora's box? *Science* **336**, 434–440 (2012). doi:10.1126/science.1215368 Medline

34. C. J. Hawker, K. L. Wooley, The convergence of synthetic organic and polymer chemistries. *Science* **309**, 1200–1205 (2005). doi:10.1126/science.1109778 Medline

35. J.-E. Haugen, O. Tomic, K. Kvaal, A calibration method for handling the temporal drift of solid state gas-sensors. *Anal. Chim. Acta* **407**, 23–39 (2000). doi:10.1016/S0003-2670(99)00784-9

36. C. S. Sample, E. A. Kellstedt, M. A. Hillmyer, Tandem ROMP/hydrogenation approach to hydroxy-telechelic linear polyethylene. *ACS Macro. Lett.* **11**, 608–614 (2022). doi:10.1021/acsmacrolett.2c00144

37. S. Kobayashi, L. M. Pitet, M. A. Hillmyer, Regio- and stereoselective ring-opening metathesis polymerization of 3-substituted cyclooctenes. *J. Am. Chem. Soc.* **133**, 5794–5797 (2011). doi:10.1021/ja201644v Medline

38. M. A. R. de Geus, G. J. M. Groenewold, E. Maurits, C. Araman, S. I. van Kasteren, Synthetic methodology towards allylic *trans*-cyclooctene-ethers enables modification of carbohydrates: Bioorthogonal manipulation of the *lac* repressor. *Chem. Sci.* **11**, 10175–10179 (2020). doi:10.1039/D0SC03216F Medline

39. G. B. Galland, R. F. de Souza, R. S. Mauler, F. F. Nunes, 13C NMR Determination of the Composition of Linear Low-Density Polyethylene Obtained with [η3-Methallyl-nickel-diimine]PF6 Complex. *Macromolecules* **32**, 1620–1625 (1999). doi:10.1021/ma981669h

40. J. Brandrup, E. H. Immergut, E. A. Grulke, *Polymer handbook*. (Wiley, ed. 4, 2003).

41. H. P. Wang, D. U. Khariwala, W. Cheung, S. P. Chum, A. Hiltner, E. Baer, Characterization of Some New Olefinic Block Copolymers. *Macromolecules* **40**, 2852–2862 (2007). doi:10.1021/ma061680e

42. H. P. Wang, S. P. Chum, A. Hiltner, E. Baer, Comparing elastomeric behavior of block and random ethylene-octene copolymers. *J. Appl. Polym. Sci.* **113**, 3236–3244 (2009). doi:10.1002/app.30070

43. M.-H. Kim, P. J. Phillips, J. S. Lin, The equilibrium melting points of random ethylene-octene copolymers: A test of the Flory and Sanchez–Eby theories. *J. Polym. Sci., B, Polym. Phys.* **38**, 154–170 (2000). doi:10.1002/(SICI)1099-0488(20000101)38:1<154:AID-POLB19>3.0.CO;2-1

44. *DOW's INFUSE Olefin Block Copolymers Product Selection Guide*, form no. 400-00130293en, The Dow Chemical Company (2009); https://www.dow.com/content/dam/dcc/documents/en-us/catalog-selguide/788/788-08201-01-infuse-olefin-block-copolymers-selection-guide.pdf (accessed 15 June 2023).

45. *ENGAGE™ Polyolefin Elastomer: Product Selection Guide*, form no. 777-088-01E-0819, The Dow Chemical Company; https://www.dow.com/content/dam/dcc/documents/en-us/catalog-selguide/777/777-088-01-engage-polyolefin-elastomer-product-selection-guide.pdf?iframe=true (accessed 15 June 2023).

46. *PETILEN YY S0464 High Density Polyethylene (HDPE)*, Petkim Petrochemical Holding Inc.; https://www.chemorbis.com/marketplace/tmDocument.do?method=showTmDoc&tmProductSpecId=1281 (accessed 15 June 2023).

47. Y. Na, S. Dai, C. Chen, Direct synthesis of polar-functionalized linear low-density polyethylene (LLDPE) and low-density polyethylene (LDPE). *Macromolecules* **51**, 4040–4048 (2018). doi:10.1021/acs.macromol.8b00467

48. *DOW ELITE™ 5940G Technical Data Sheet*, form no. 400-00130293en, The Dow Chemical Company (2009); https://www.dow.com/en-us/document-viewer.html?docPath=/content/dam/dcc/documents/en-us/productdatasheet/400-1/400-00130293en-elite-5940g-tds.pdf (accessed 15 Jun 2023).

49. F. C. Stehling, L. Mandelkern, The glass temperature of linear polyethylene. *Macromolecules* **3**, 242–252 (1970). doi:10.1021/ma60014a023

50. R. F. Boyer, Glass temperatures of polyethylene. *Macromolecules* **6**, 288–299 (1973). doi:10.1021/ma60032a029

51. H. E. Park, J. M. Dealy, G. R. Marchand, J. Wang, S. Li, R. A. Register, Rheology and structure of molten, olefin multiblock copolymers. *Macromolecules* **43**, 6789–6799 (2010). doi:10.1021/ma1012122

52. B. Patham, K. Jayaraman, Creep recovery of random ethylene-octene copolymer melts with varying comonomer content. *J. Rheol. (N.Y.N.Y.)* **49**, 989–999 (2005). doi:10.1122/1.2008296